

Modern Astronomy

Part 1. Interstellar Medium (ISM)

Week 4

March 28 (Tuesday), 2022

updated 03/21, 20:51

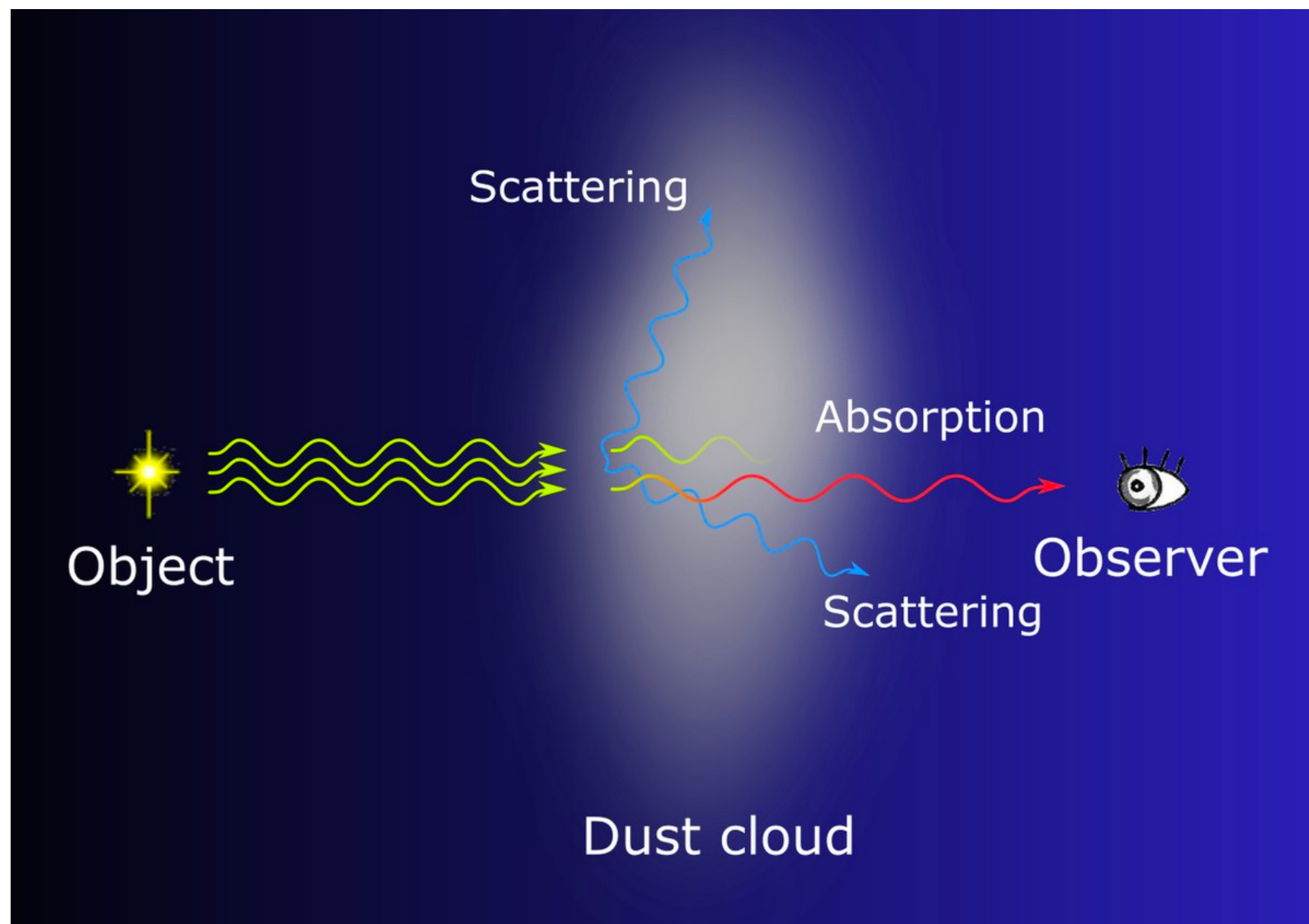
선광일 (Kwang-Il Seon)

UST / KASI

Reddening

- ***Reddening***

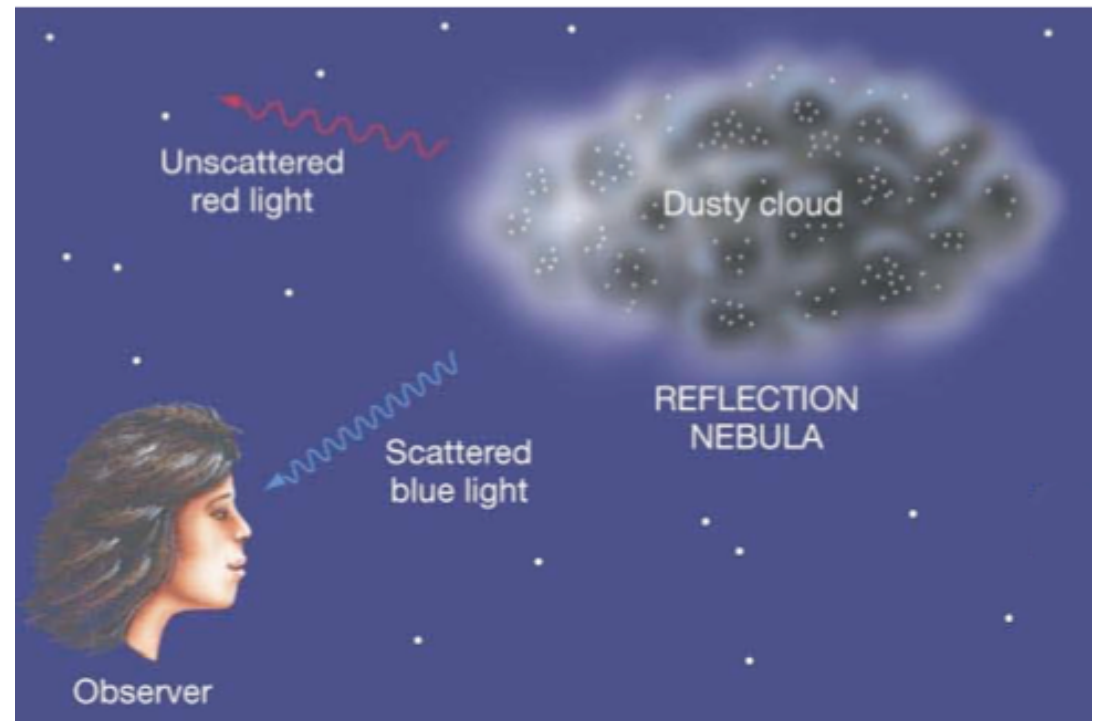
- Reddening is the phenomena of the color of a visible astronomical object (e.g., star) appearing more red from a distance than from nearby. Within the visible wavelength range, the absorption/scattering by dust increases with frequency, absorbing/scattering more of the blue light than red. This effect leads to the reddening.



Blue Reflection Nebulae

- ***Scattering of Starlight***

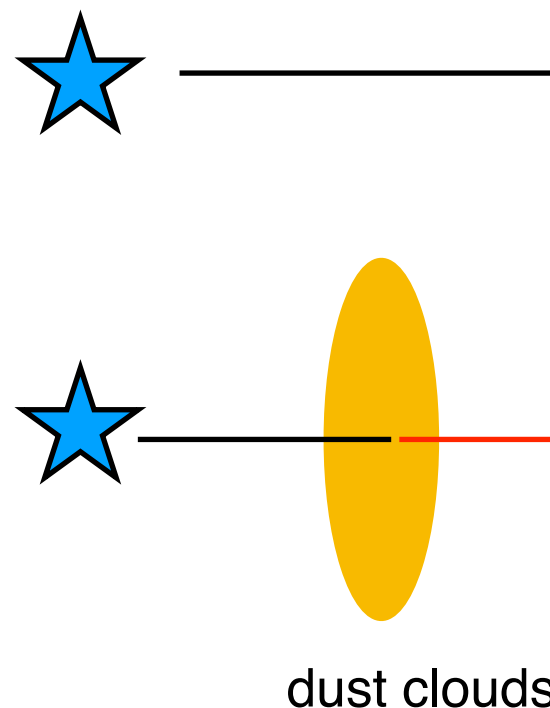
- When an interstellar cloud happens to be unusually near one or more bright stars, we have a reflection nebula, where we see starlight photons that have been scattered by the dust in the cloud.
- ***The spectrum of the light coming from the cloud surface shows the stellar absorption lines***, thus demonstrating that scattering rather than some emission process is responsible.
- Given the typical size of interstellar dust grains, blue light is scattered more than red light. ***A reflection nebulae is typically blue*** (so for the same reason that the sky is blue, except it's scattering by dust (for the reflection nebula) vs by molecules (for the earth's atmosphere)).



How to measure the Interstellar Extinction

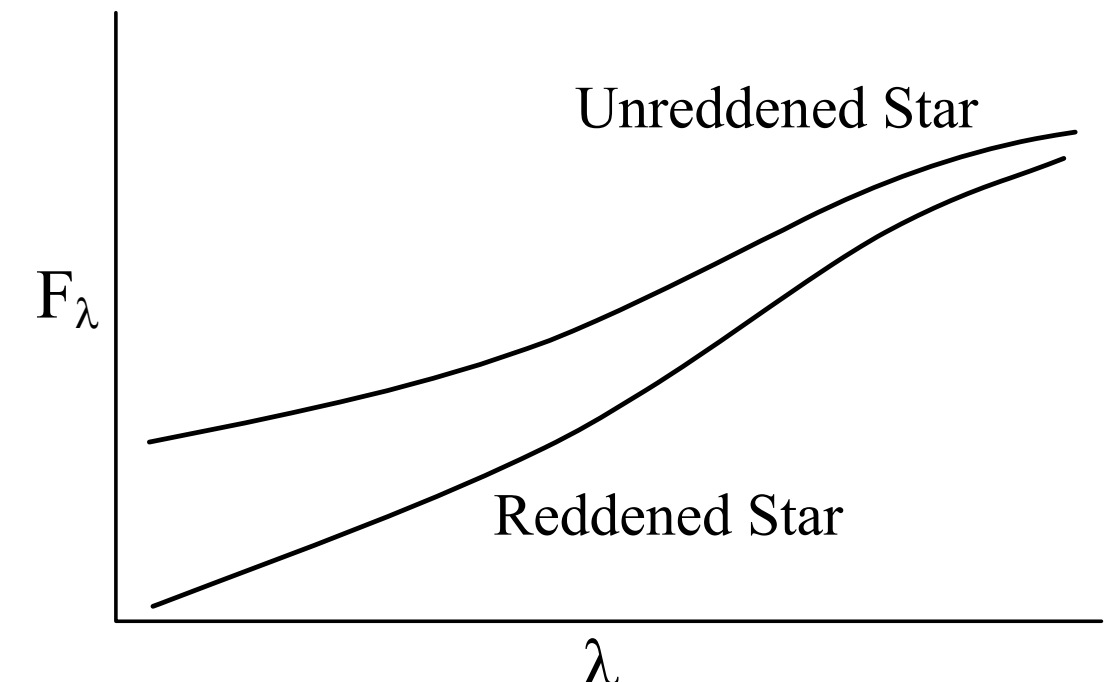
- Pair method
 - Trumpler (1930) compared the spectra of pairs of stars with identical (or similar) spectral type, one with negligible obscuration and the other extinguished by dust along the line of sight. This method remains our most direct way to study the “selective extinction” or “reddening” of starlight by the interstellar dust.

two stars
with the same spectral type



$$F(\lambda) = \frac{F_0(\lambda)}{4\pi d_1^2}$$

$$F(\lambda) = \frac{F_0(\lambda)}{4\pi d_2^2} e^{-\tau_\lambda}$$



- ***The Reddening Law, Extinction Curve***

- Extinction curve - the extinction A_λ as a function of wavelength or frequency
 - ▶ A typical extinction curve shows the ***rapid rise in extinction in the UV.***
 - ▶ ***The extinction increases from red to blue,*** and thus the light reaching us from stars will be “reddened” owing to greater attenuation of the blue light.
 - ▶ The reddening by dust is expressed in terms of a color excess; for instance,

B-V color excess:

$$E(B - V) \equiv A_B - A_V$$

$$\begin{aligned}\lambda_B &\sim 4400 \text{ \AA} \\ \lambda_V &\sim 5500 \text{ \AA}\end{aligned}$$

in general,

$$E(\lambda_1 - \lambda_2) \equiv A_{\lambda_1} - A_{\lambda_2} \quad (\lambda_1 < \lambda_2)$$

- ▶ The detailed wavelength dependence of the extinction - the “reddening law” - is sensitive to the composition and size distribution of the dust particles.
- ▶ The slope of the extinction at visible wavelengths is characterized by the dimensionless ratio, the ratio of total to selective extinction:

$$R_V \equiv \frac{A_V}{A_B - A_V} \equiv \frac{A_V}{E(B - V)}$$

- ▶ R_V ranges between 2 and 6 for different lines of sight. Sightlines through diffuse gas in the Milky Way have $R_V \approx 3.1$ as an average value. ***Sightlines through dense regions tend to have larger values of R_V .*** In dense clouds, the value $R_V \approx 5$ is typically adopted.

- ▶ ***Observed extinction curves vary in shape from one line of sight to another.***
- ▶ Extinction curve, relative to the extinction in the I band ($\lambda = 8020\text{\AA}$), as a function of inverse wavelength, for Milky Way regions characterized by different values of R_V .

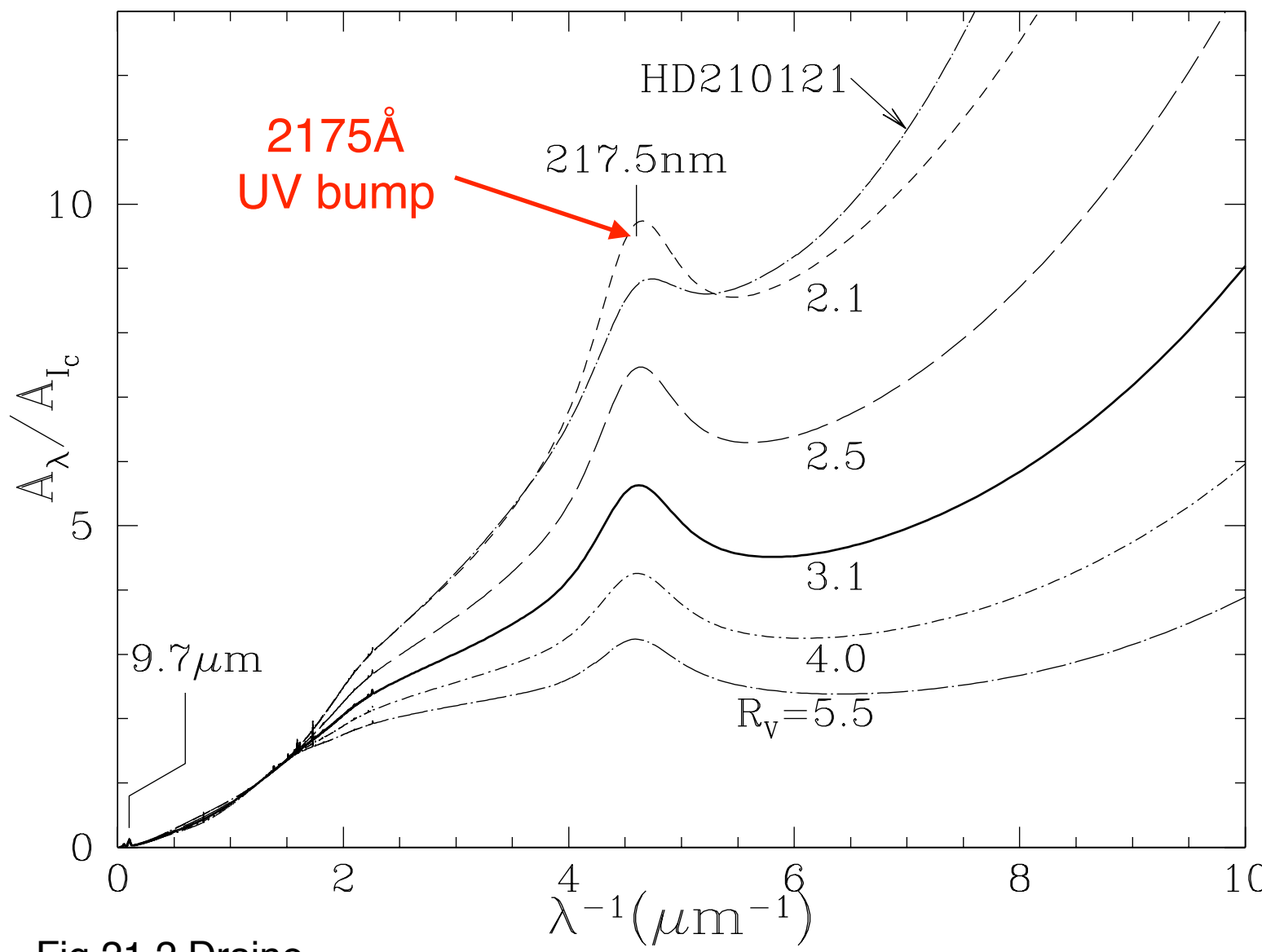


Fig 21.2 Draine

Parameterization of the extinction curve.

Cardelli et al. (1989)

Fitzpatrick (1999)

Gas-to-dust ratio

- If the dust grains were large compared to the wavelength, we would be in the “geometric optics” limit, and the extinction cross section would be independent of wavelength (gray extinction).
 - ▶ The tendency of the extinction to rise with decreasing λ , even at the shortest ultraviolet wavelengths tells us that grains smaller than the wavelength must be making an appreciable contribution to the extinction at all observed wavelengths, down to $\lambda = 0.1 \mu\text{m}$.
 - ▶ According to the Mie theory, “small” means (approximately) that $2\pi a/\lambda \lesssim 1$. Thus interstellar dust must include a large population of small grains with $a \lesssim 0.015 \mu\text{m}$.
- The dust appears to be relatively well-mixed with the gas (Bohlin et al. 1978; Rachford et al. 2009):

$$\frac{N_{\text{H}}}{E(B-V)} = 5.8 \times 10^{21} \text{ H cm}^{-2} \text{ mag}^{-1}$$

- ▶ For sightlines with $R_V \approx 3.1$, this implies that

$$\frac{A_V}{N_{\text{H}}} \approx 5.3 \times 10^{-22} \text{ mag cm}^2 \text{ H}^{-1}$$

column density of total hydrogen nuclei
 $N_{\text{H}} \equiv N(\text{HI}) + 2N(\text{H}_2)$

- ▶ Thus, even at high galactic latitudes, where the column density of hydrogen is $\sim 10^{20} \text{ cm}^{-2}$, there is still some foreground extinction when looking at extragalactic sources; ~ 0.05 magnitudes in the V band.
- ***Mean ratio of visual extinction to length in the Galactic plane***

$$\left\langle \frac{A_V}{L} \right\rangle \approx 1.8 \text{ mag kpc}^{-1}$$

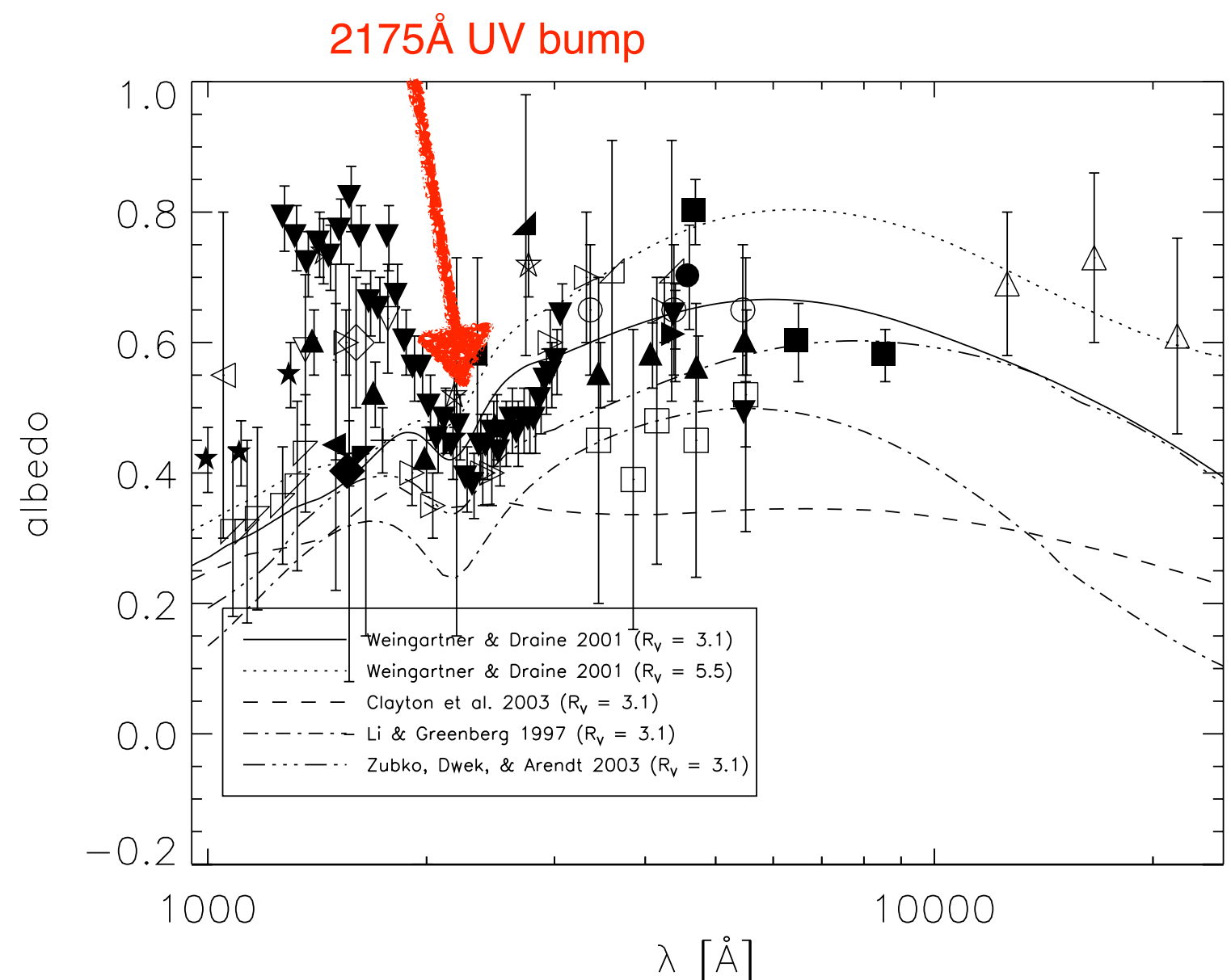
UV bump

- The study of dust scattering properties has shed light on the nature of the 2175Å bump and the far-ultraviolet rise features of extinction curves.
- Lillie & Witt (1976) and Calzetti et al. (1995) showed that ***the 2175Å bump was likely an absorption feature with no scattered component.***

The determinations of the albedo in reflection nebulae, dark clouds, and the diffuse Galactic light are plotted versus wavelength.

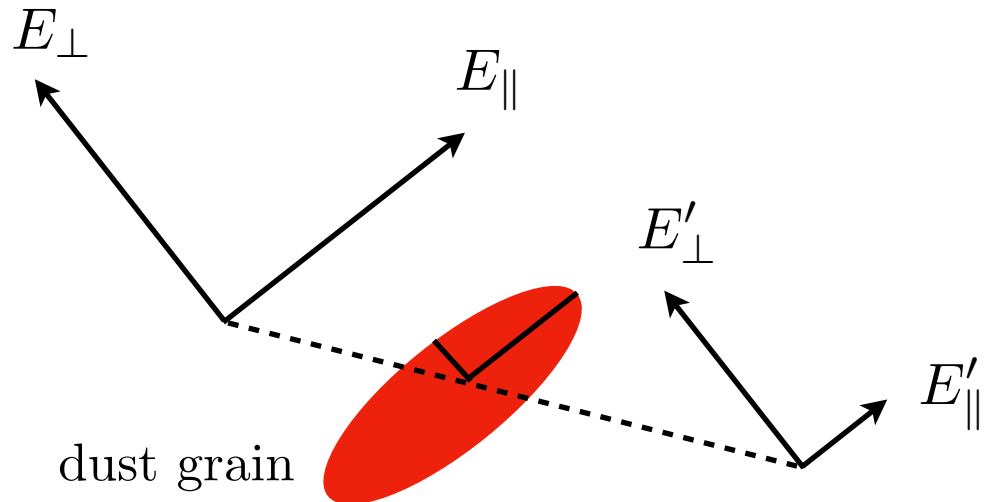
Predictions from dust grain models are also plotted for comparison.

Karl D. Gordon,
2004, ASPC, 309, 77



- **Polarization of Starlight by Interstellar Dust**

- Initially unpolarized light propagating through the ISM becomes linearly polarized as a result of ***preferential extinction*** of one linear polarization mode relative to the other.



$$E_{\parallel} = E_{\perp}$$

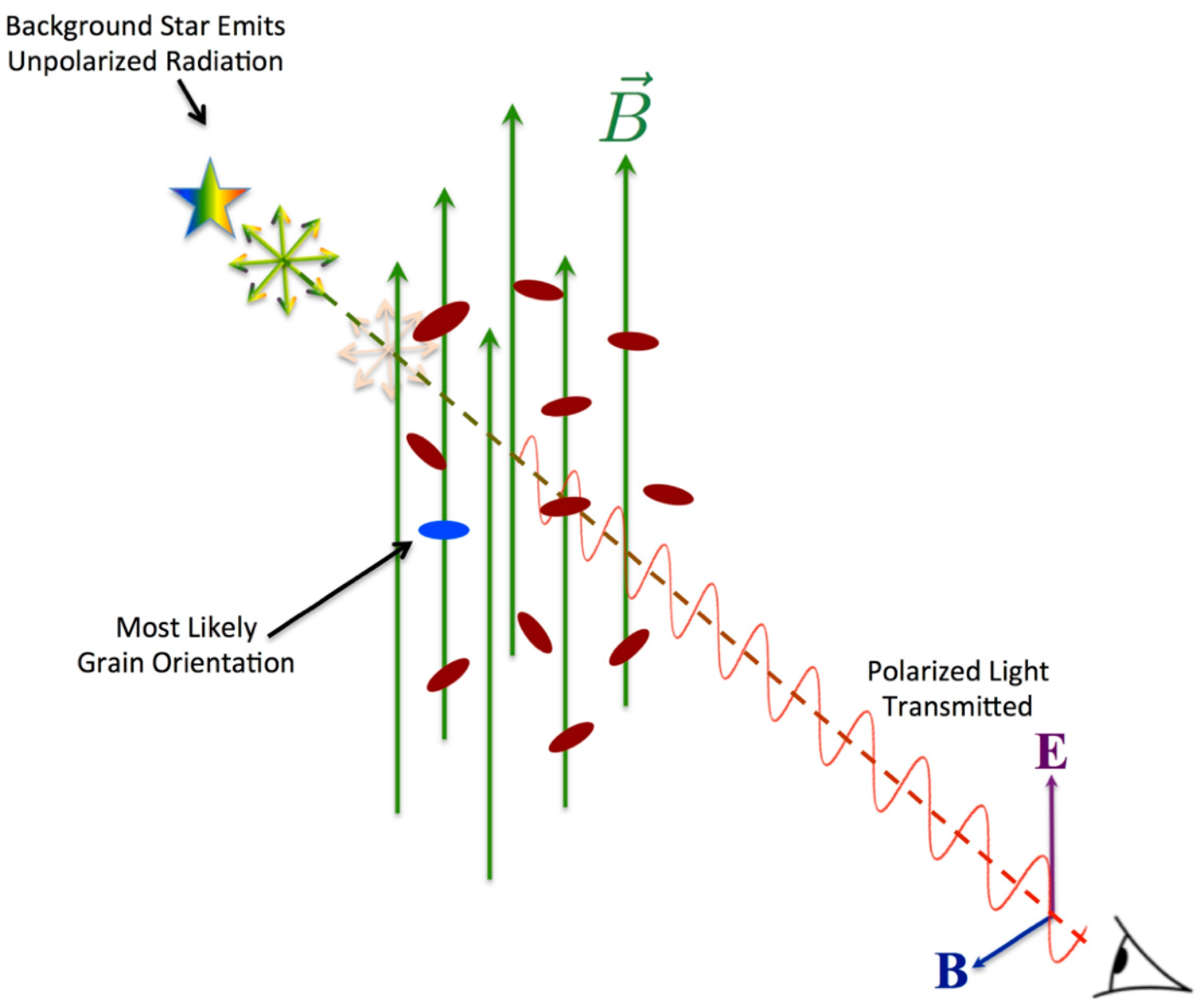
$$E'_{\parallel} < E'_{\perp}$$

$$E'_{\parallel} = E_{\parallel} e^{-\tau_{\parallel}}$$

$$E'_{\perp} = E_{\perp} e^{-\tau_{\perp}}$$

$$\tau_{\parallel} > \tau_{\perp}$$

The starlight is slightly more blocked along the long axis of the grains than along the short axis. This give rise to the polarization of starlight.



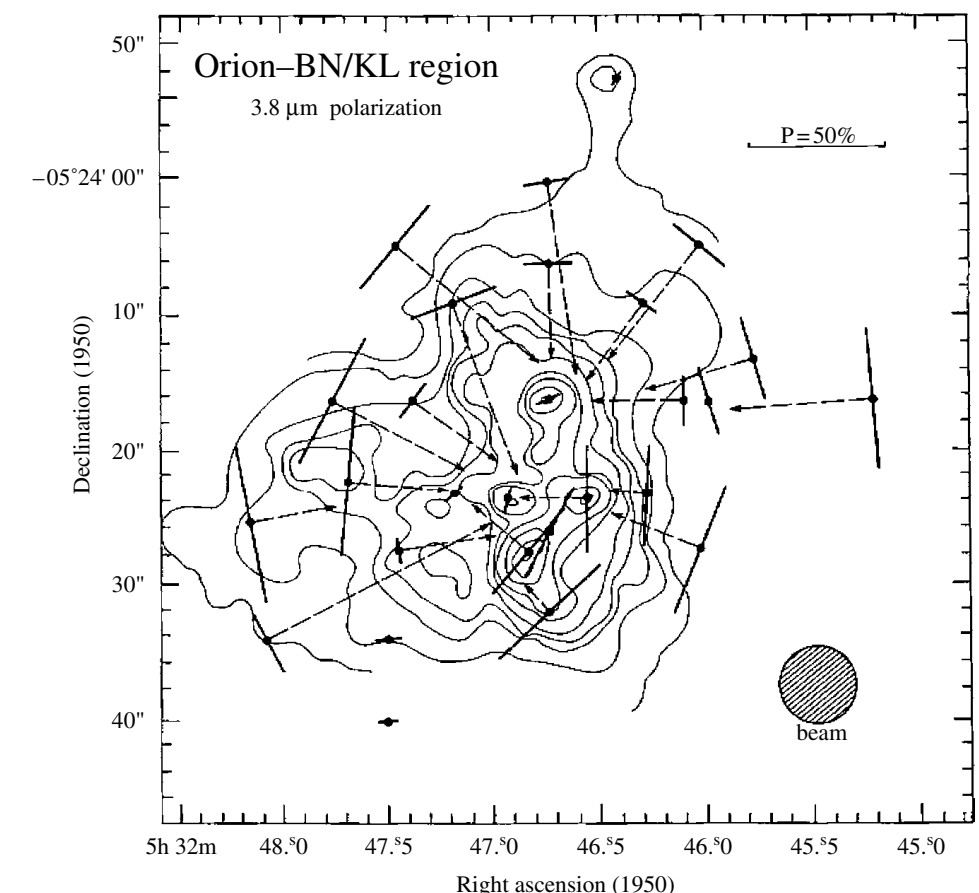
credit: B-G Andersson

- **Polarized Infrared Emission**

- The far-IR emission from aligned dust grains will also be polarized, this time with a direction along the long axis of the grains. Far-IR polarization has been observed for a large number of molecular clouds that have “high” dust emission optical depths at long wavelengths ($\sim 0.1\text{-}1$ mm).

- **Polarization due to scattering**

- Scattering of light by dust grains generally also lead to polarization.
- For single scattering, the polarization vector is perpendicular to the line connecting the light source and the scattering grain.
- The degree of polarization and its distribution provide information on the characteristics of the scattering grains and the geometry of the nebula.



Linear polarization of the IR reflection nebula associated with the region of massive star formation in Orion.

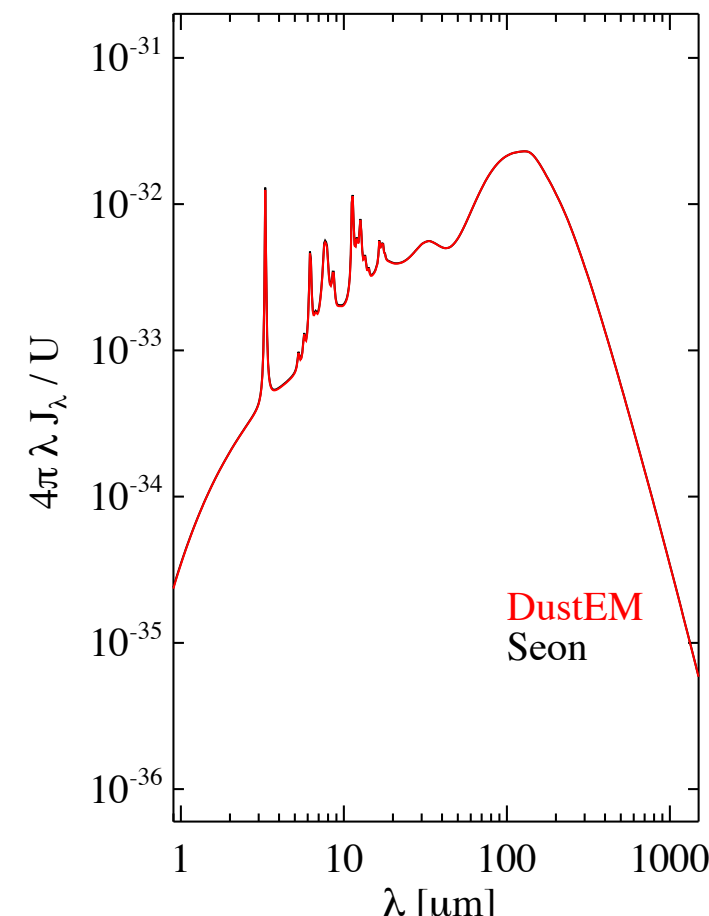
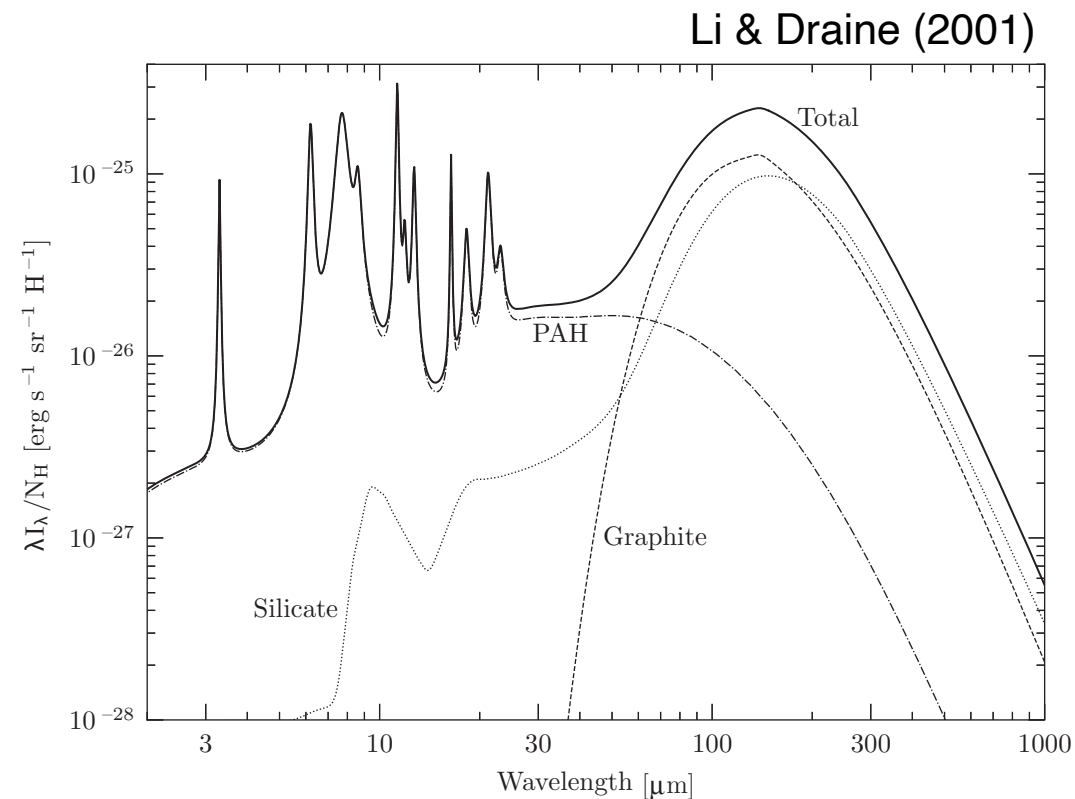
The linear polarization vectors measured at K are superimposed on a map of the scattered light intensity.

[Werner et al. 1983, ApJ, 265, L13]

Infrared Emission

- ***Infrared Emission***

- Dust grains are heated by starlight, and cool by radiating in the infrared.
- The IR spectrum provides very strong constraints on grain models.
- There are two components: ***a cold ($T \sim 15\text{-}20 K$) component*** emitting mainly at long wavelengths (far-IR) and ***a hot ($T \sim 500 K$) component*** dominating the near- and mid-IR emission.
 - ▶ The **cold component** is due to **large dust grains** in radiative equilibrium with the interstellar radiation field.
 - ▶ The **hot component** is due to **ultra small grains and PAH species** that are heated by a single UV photon to temperatures of $\sim 1000 K$ and cool rapidly in the near- and mid-IR.



What are the dust grains made of?

- Observational Constraints
 - **Interstellar Depletion:** Certain elements appear to be underabundant or “depleted” in the gas phase. The observed depletions tell us about the major elemental composition of interstellar dust.
 - **Spectroscopy:** We would observe spectroscopic features that would uniquely identify the materials, and allow us to measure the amounts of each material present.
But, it is difficult to apply this approach to solid materials because: (1) the optical and UV absorption is largely a continuum; and (2) the spectral features are broad, making them difficult to identify conclusively.
 - **Extinction:**
 - ▶ The wavelength dependence of the extinction curve provides constraints on the interstellar grain size distribution.
 - ▶ What materials could plausibly be present in the ISM in quantities sufficient to account for the observed extinction? A Kramers-Kronig integral over the observed extinction indicates that the total grain mass relative to total hydrogen mass:

$$M_{\text{dust}}/M_{\text{H}} \gtrsim 0.0083$$

Interstellar Depletion

- Condensable elements:
 - ▶ Hydrogen: There is no way to have hydrogen contribute appreciably to the grain mass (even polyethylene (CH_2)_n is 86% carbon by mass).
 - ▶ The noble gases (He, Ne, Ar, Kr, Xe...) and nitrogen(N), zinc (Zn), and sulfur (S) are examples of species that generally form only rather volatile (휘발성) compounds. They are observed to be hardly depleted at all.
volatile = easily evaporated at normal temperature
 - ▶ The only way to have a dust/H mass ratio of 0.0056 or higher is to build the grains out of the most abundant condensable elements: C, O, Mg, Si, S, and Fe (refractory materials; 내열성물질).
refractory = stubborn or unmanageable
- Abundance Constraints toward ζ Oph
 - ▶ Nitrogen is present at its solar abundance.
 - ▶ C abundance is at $\sim 35\%$ of its solar value.
 - ▶ O abundance is at $\sim 55\%$ of its solar value.
 - ▶ Mg is at $\sim 11\%$.
 - ▶ Si is at $\sim 5\%$.
 - ▶ Fe is at $\sim 0.4\%$.

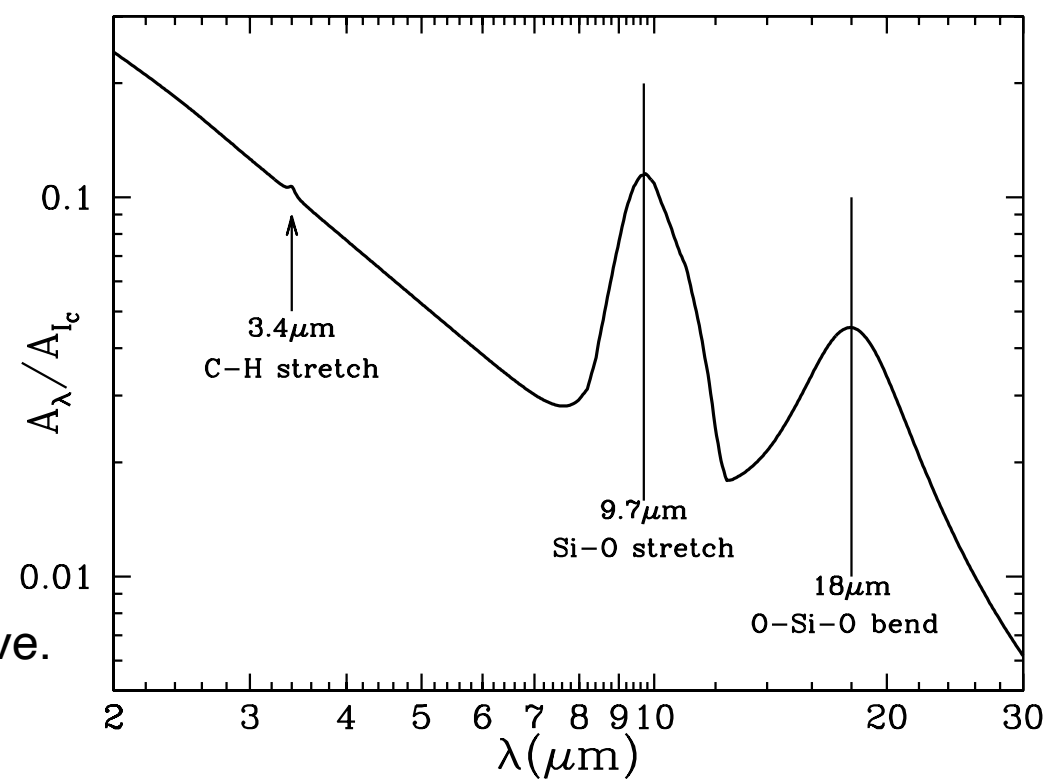
Observed Spectral Features of Dust

- The 2175Å Feature (UV bump)
 - The strongest feature in the interstellar extinction curve is a broad “bump” centered at $\sim 2175\text{\AA}$ where there is additional absorption above the rough $1/\lambda$ behavior at adjacent wavelengths.
 - ▶ The feature is well-described by a **Drude profile**.
- $$S(\lambda) = \frac{2}{\pi} \frac{\gamma_0 \lambda_0 \sigma_{\text{int}}}{(\lambda/\lambda_0 - \lambda_0/\lambda)^2 + \gamma_0^2} \quad \text{where } \sigma_{\text{int}} = \int S(\lambda) d\lambda^{-1}$$
- ▶ The central wavelength is nearly identical on all sightlines, but the width varies significantly from one region to another.
 - ▶ The strength of the feature is a strong function of the metallicity of the gas, with the UV bump appearing slightly weaker in the LMC extinction curve (metallicity $\sim 50\%$ solar), but essentially absent in the SMC extinction curve (metallicity $\sim 10\%$ solar).
 - The strength of this feature implies that the responsible material must be abundant: it must be made of H, C, N, O, Mg, Si, S, or Fe.

- Mid-Infrared Silicate Features:

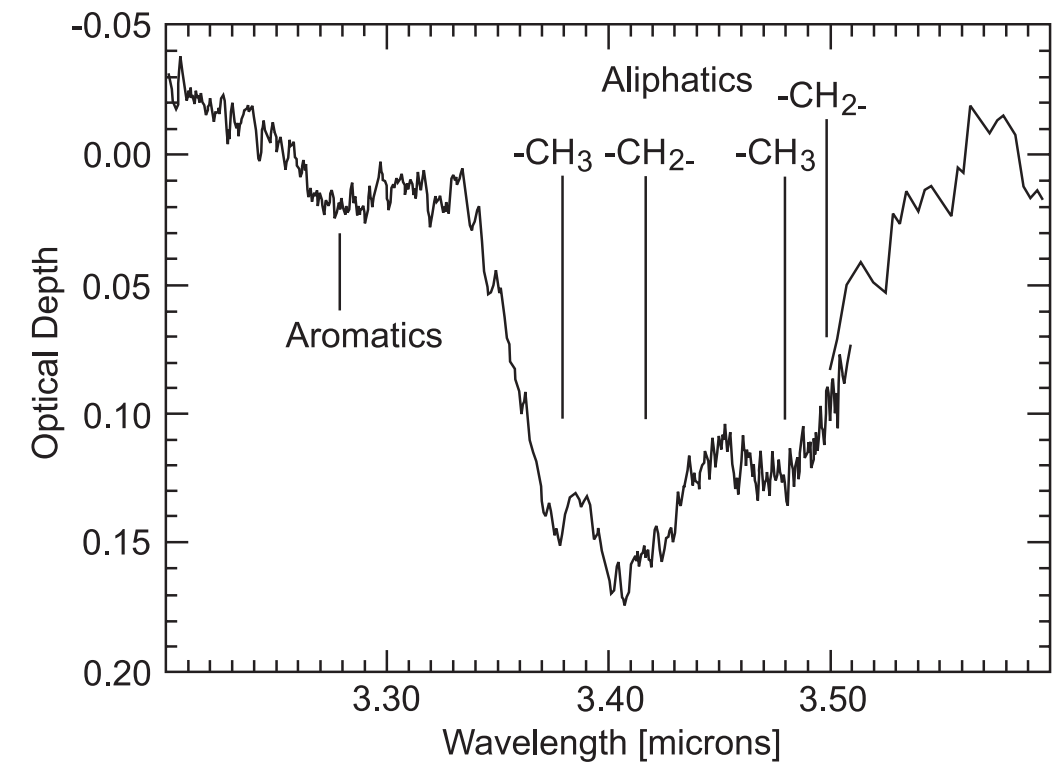
The fact that the $9.7\mu\text{m}$ band is fairly featureless, unlike what is seen in laboratory silicate crystals, suggests that this “astrophysical” silicate is primarily amorphous rather than crystalline in nature.

IR extinction curve.
[Fig 23.2 Draine]



- The $3.4\mu\text{m}$ Feature

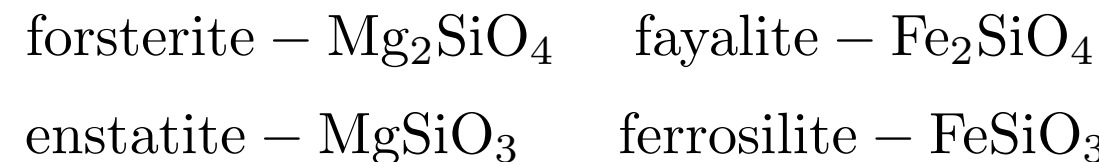
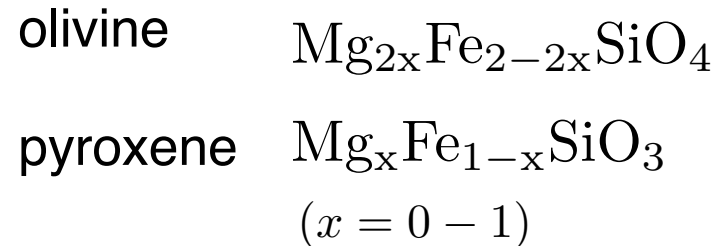
- There is a broad absorption feature at $3.4\mu\text{m}$ that is almost certainly due to the C-H stretching mode in “aliphatic” hydrocarbons (organic molecules with carbon atoms joined in straight or branched chains).



The source GCS3 in the
Galactic Center
Chiar et al. (2000, ApJ)

Dust Materials

- Silicates
 - The two main types of silicates in dust are pyroxene and olivine.



[Left] Olivine is the simplest silicate structure, which is composed of isolated tetrahedra bonded to iron and/or magnesium ions. No oxygen atom is shared to two tetrahedra.

[Middle] In pyroxene, silica tetrahedra are linked together in a single chain, where one oxygen ion from each tetrahedra is shared with the adjacent tetrahedron.

[Right] Other types are possible. In amphibole structures, two oxygen ions from each tetrahedra are shared with the adjacent tetrahedra.

In mica structures, the tetrahedra are arranged in continuous sheets, where each tetrahedron shares three oxygens with adjacent tetrahedra.

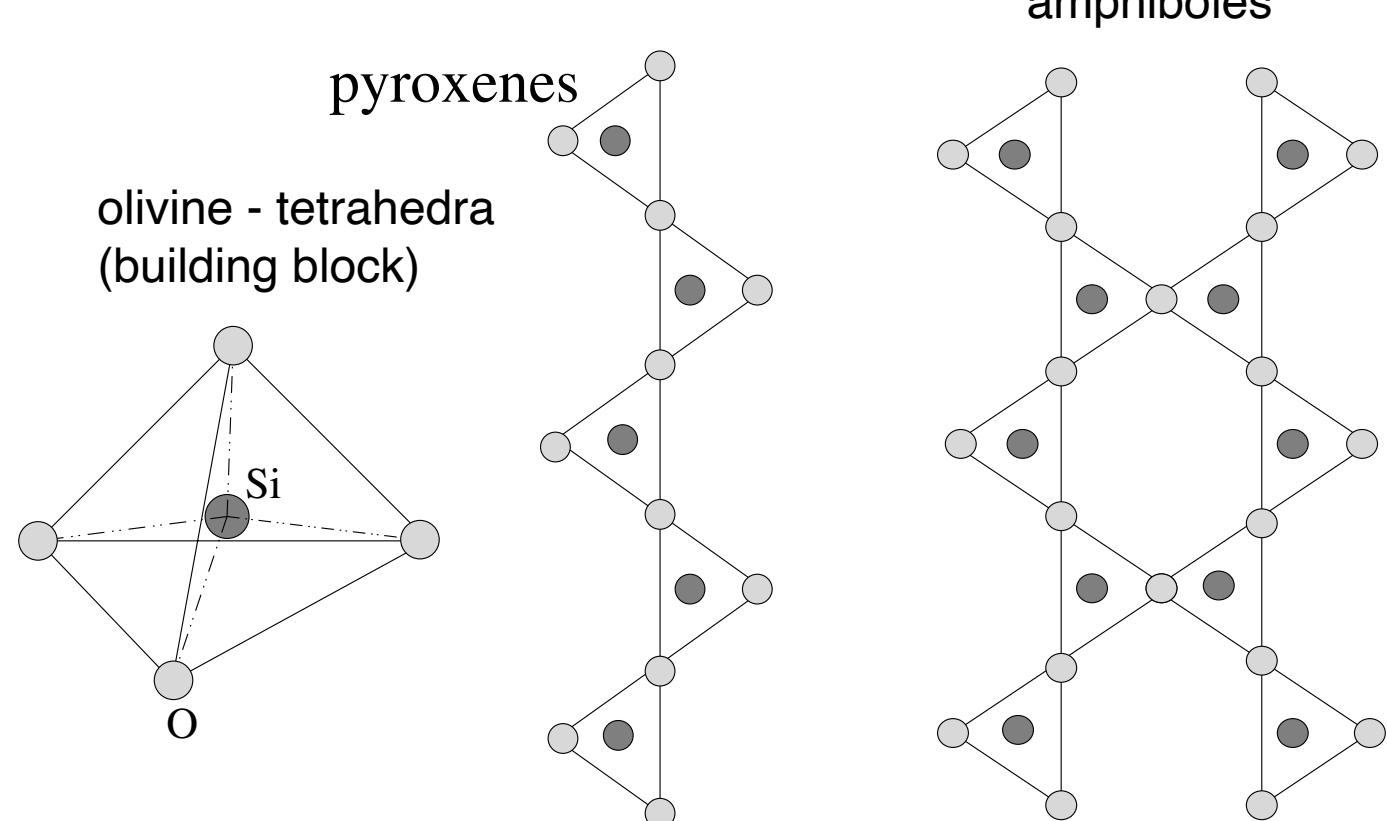
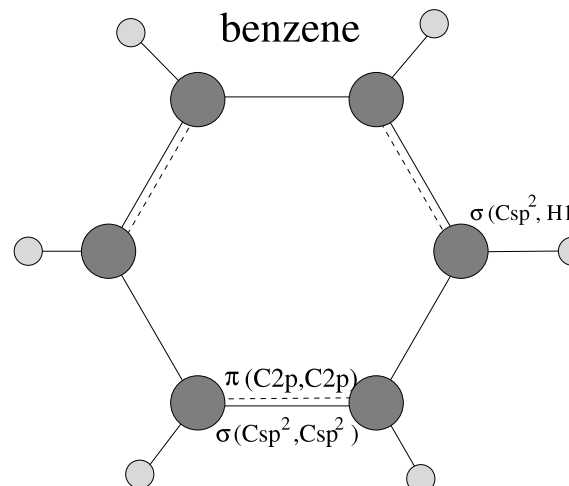


Fig 5.9 Krugel
[An Introduction to the Physics of Interstellar Dust]

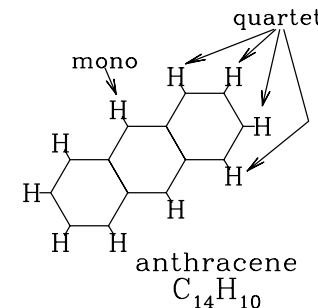
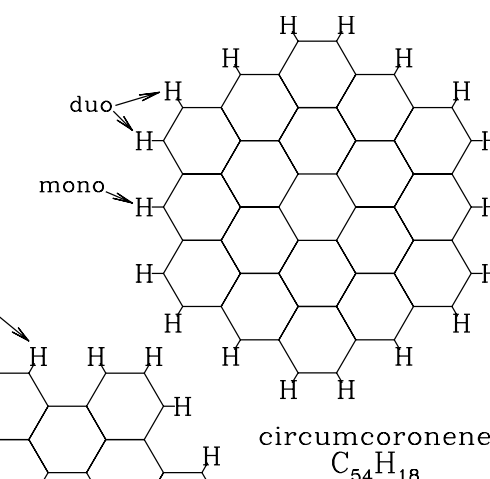
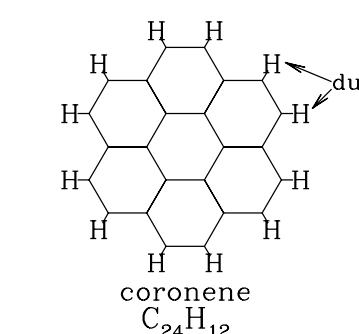
• Polycyclic Aromatic Hydrocarbons

- The IR emission spectra of spiral galaxies show emission features at 3.3, 6.2, 7.7, 8.6, 11.3, and 12.7 μm that are attributable to vibrational transitions in polycyclic aromatic hydrocarbon (PAH) molecules.
- PAH molecules are planar structures consisting of carbon atoms organized into hexagonal rings, with hydrogen atoms attached at the boundary.

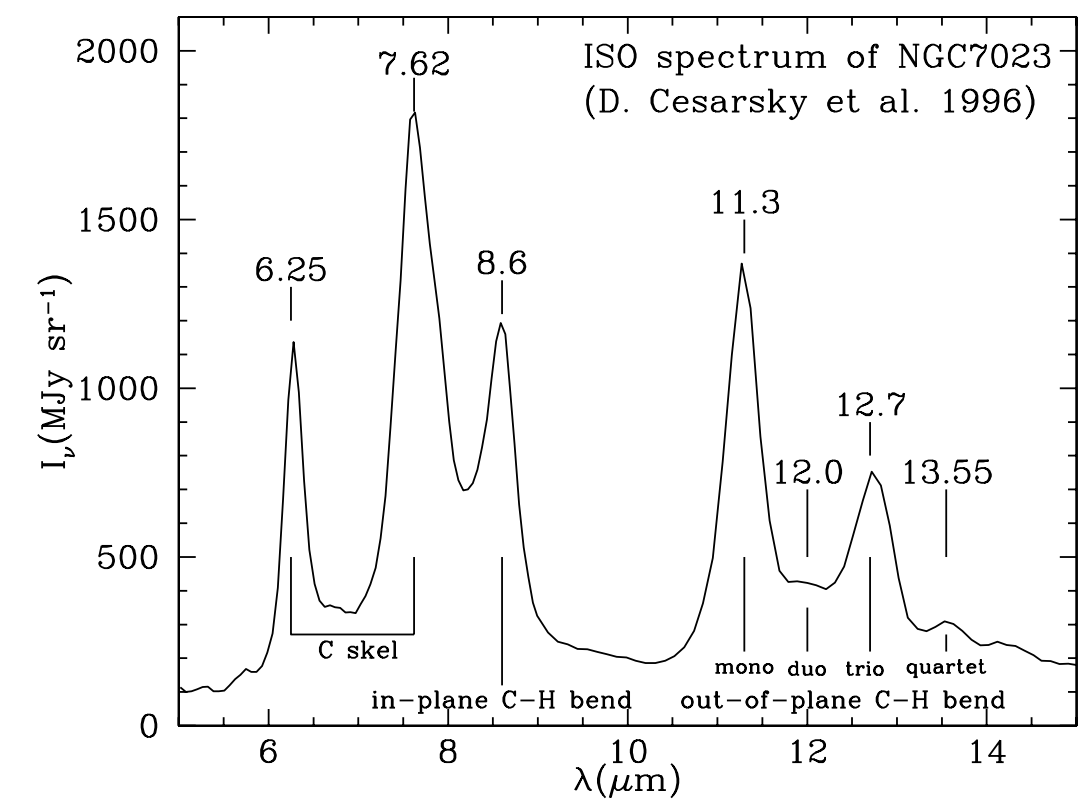


Bezene ring:
The simplest type of PAHs.

[Fig 5.6 in Krugel]



Structure of four PAHs.
[Fig 23.9 in Draine]



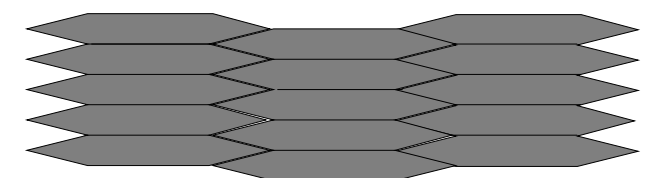
The IR spectrum of the reflection nebula NGC 7023 (Cesarsky et al. 1996)

- Graphite (흑연)

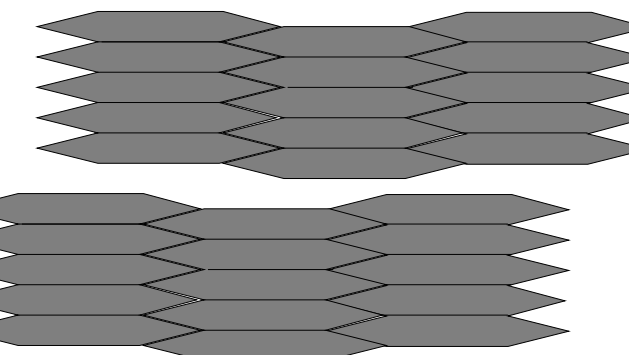
- Graphite is the most stable form of carbon (at low pressure), consisting of infinite parallel sheets of sp^2 -bonded carbon.
 - ▶ A single (infinite) sheet of carbon hexagons is known as graphene. Each carbon atom in graphene has three nearest neighbors, with a nearest-neighbor distance of 1.421\AA .
 - ▶ Crystalline graphite consists of regularly stacked graphene sheets.
 - ▶ The sheets are weakly bound to one another by van der Waals forces.



graphite sheets

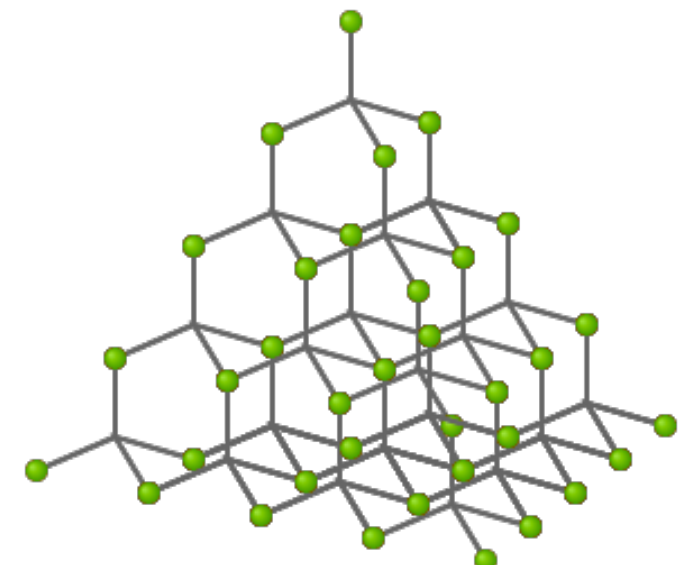


3.35\AA



- Nanodiamond

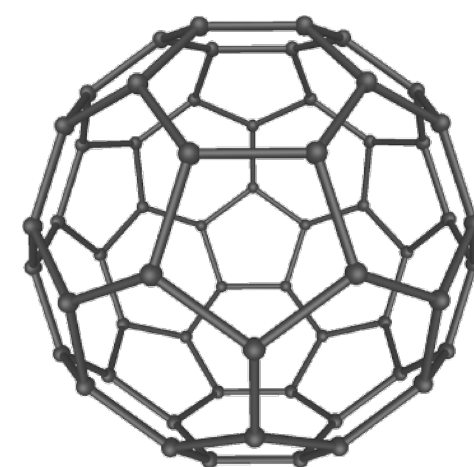
- Diamond consists of sp^3 -bonded carbon atoms, with each carbon bonded to four equidistant nearest neighbors (enclosed angles are 109.47°).
- Diamond nanoparticles are relatively abundant in primitive meteorites. Based on isotopic anomalies associated with them, we know that some fraction of the nanodiamond was of premolar origin.
- But, its abundance in the ISM is not known.



- Armorphous carbon

- Hydrogenated amorphous carbon (HAC)

- Fullerenes



Buckminsterfullerene (C_{60})

Structure of diamond.

Dust Theory: cross section and efficiency factors

- **Cross Sections:**

- A dust grain has wavelength-dependent cross sections for absorption and scattering. Extinction is the sum of absorption and scattering processes.

$$C_{\text{ext}}(\lambda) = C_{\text{abs}}(\lambda) + C_{\text{sca}}(\lambda)$$

- For a population of dust grains with number density n_d , the extinction cross section is related to the extinction coefficient and the dust optical depth by:

$$\kappa_\lambda = n_d C_{\text{ext}}(\lambda)$$

$$\begin{aligned} \tau_\lambda &= n_d C_{\text{ext}}(\lambda) L && L = \text{pathlength} \\ &= 1.086 A_\lambda \end{aligned}$$

- **Efficiency Factors:**

- The cross section is often expressed in terms of efficiency factors, normalized to the geometric cross section of an equal-solid-volume sphere:

$$Q_{\text{ext}}(\lambda) = \frac{C_{\text{ext}}(\lambda)}{\pi a^2}, \quad Q_{\text{abs}}(\lambda) = \frac{C_{\text{abs}}(\lambda)}{\pi a^2}, \quad Q_{\text{sca}}(\lambda) = \frac{C_{\text{sca}}(\lambda)}{\pi a^2}$$

$$V = \frac{4\pi}{3} a^3 \quad a = \text{the radius of an equal-volume sphere}$$

- Albedo and Scattering phase function

- The **albedo** is defined by

$$\omega(\lambda) = \frac{C_{\text{sca}}(\lambda)}{C_{\text{ext}}(\lambda)}$$

In many cases, the albedo is denoted by a or ω .

- Scattering is a function of the scattering angle and thus expressed in terms of the differential scattering cross section:

$$C_{\text{sca}}(\lambda) = \int_0^{2\pi} \int_0^\pi \frac{d\sigma_{\text{sca}}(\theta, \phi; \lambda)}{d\Omega} \sin \theta d\theta d\phi$$

- The **scattering asymmetry factor** is defined by:

$$g \equiv \langle \cos \theta \rangle = \frac{1}{\sigma_{\text{sca}}} \int_0^{2\pi} \int_0^\pi \cos \theta \frac{d\sigma_{\text{sca}}}{d\Omega} \sin \theta d\theta d\phi$$

- The scattering phase function can be described by the Rayleigh function or Henyey-Greenstein function:

$$\mathcal{P}(\theta) \equiv \frac{1}{\sigma_{\text{sca}}} \int_0^\pi \frac{d\sigma_{\text{sca}}}{d\Omega} d\phi \rightarrow$$

$\mathcal{P}_{\text{Ray}}(\theta) = \frac{1}{2} (1 + \cos^2 \theta)$ $\mathcal{P}_{\text{HG}}(\theta) = \frac{1}{2} \frac{1 - g^2}{(1 + g^2 - 2g \cos \theta)^{3/2}}$	for $\frac{2\pi a}{\lambda} \ll 1$ \longrightarrow $\langle \cos \theta \rangle = 0$	for $\frac{2\pi a}{\lambda} \gg 1$ \longrightarrow $\langle \cos \theta \rangle = g$
--	--	--

- ▶ The Henyey-Greestein phase function is only introduced for computational convenience and has no physical meaning.

Theoretical Model of the Extinction Curve

- Scattering Theory: How to calculate the theoretical extinction curve.
 - **Mie scattering** (Gustave Mie), the general solution for (absorbing or non-absorbing) spherical particles without a particular bound on particle size. ==> complex
- A model for interstellar dust must specify the **composition** of the dust as well as the geometry (**shape and size**) of the dust particles.
 - If the model is to reproduce the polarization of starlight, at least some of the grains should be nonspherical and aligned.
 - However, it is not yet possible to arrive at a unique grain model.

Models for Interstellar Dust

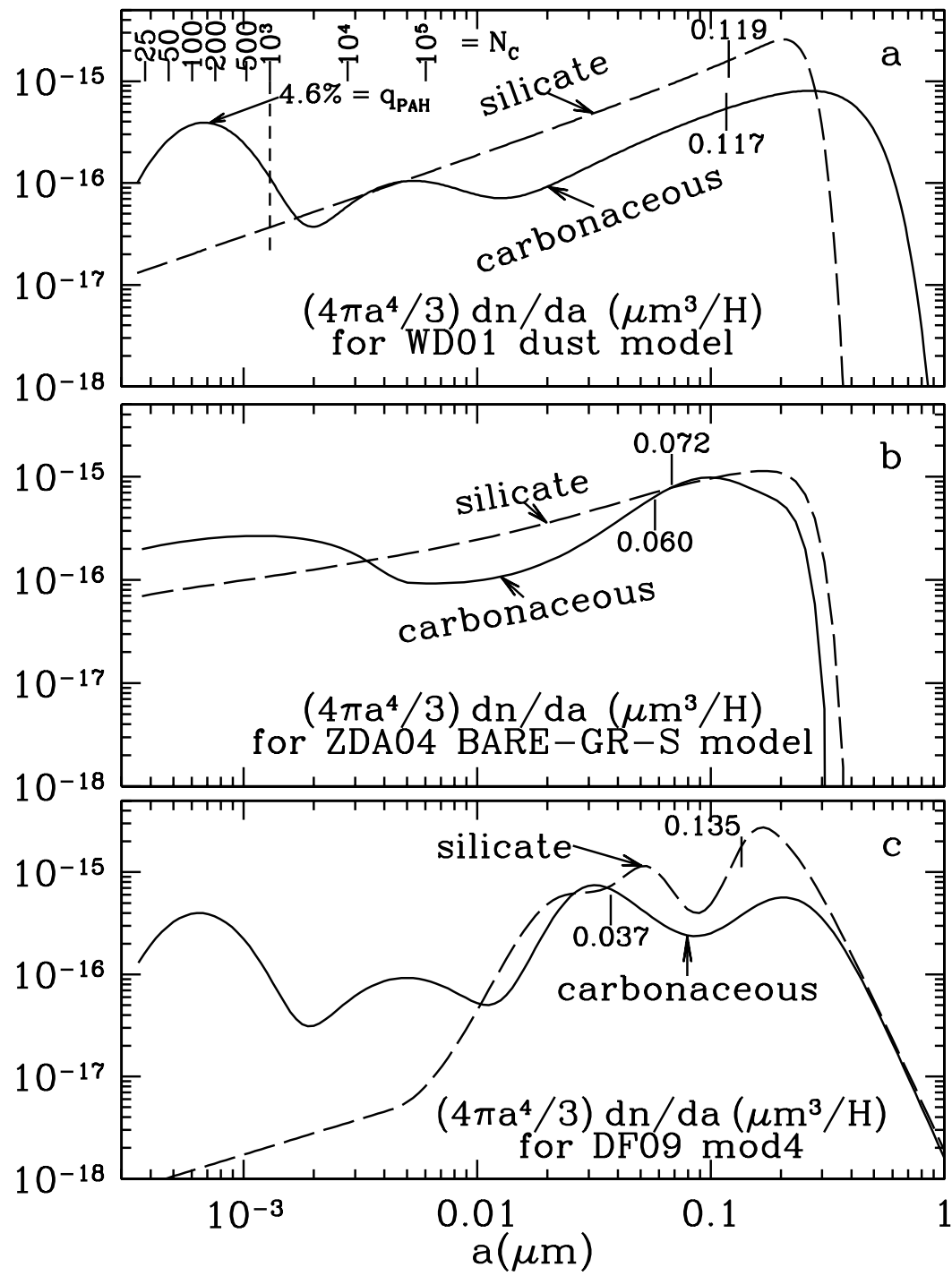
- A class of models that has met with some success assumes the dust to consist of two materials: (1) amorphous silicate, and (2) carbonaceous material.
 - ***Mathis, Rumpl, and Nordsieck (1977; MRN)*** found that models using two components, silicate and graphite spheres with power-law size distributions, could reproduce the observed extinction from the near-IR to the UV ($\lambda = 0.11\mu\text{m} - 1\mu\text{m}$).

$$\frac{dn_{\text{gr}}}{da} da = A_i n_{\text{H}} a^{-3.5} da \quad \text{for } a_{\min} \leq a \leq a_{\max}$$

$a_{\min} \approx 0.025\mu\text{m}$
 $a_{\max} \approx 0.25\mu\text{m}$

$$A_{\text{sil}} = 7.8 \times 10^{-26}, \quad A_{\text{gra}} = 6.9 \times 10^{-26} \text{ cm}^{2.5} (\text{H atom})^{-1}$$

- ▶ Graphite was a necessary component. The other could be silicon carbide (SiC), magnetite (Fe_3O_4), iron, olivine, or pyroxene.
- ***Draine and Collaborators***
 - ▶ Draine & Lee (1984) presented self-consistent dielectric functions for graphite and silicate, and showed that the graphite-silicate model appeared to be consistent with what was known about dust opacities in the Far-IR. (extended the MRN model to the Far-IR).
- ***Zubko et al. (2004)***
 - ▶ The size distribution of the “BARE-GR-S” model of Zubko et al. (2004), composed of bare graphite grains, bare silicate grains, and PAHs, differs significantly from the WD01 size distribution.



A “typical” grain size may be taken as the half-mass grain size $a_{0.5}$, defined so that half the mass of dust is in grains of radius $a_{0.5}$ or greater.

Size distributions for silicate and carbonaceous grains for dust models from (a) Weingartner & Draine (2001), (b) Zubko et al. (2004), and (c) Draine & Faisse (2009).

In each case, tick-marks indicate the “half-mass” radii for the silicate grains and carbonaceous grains.

[Fig 23.10 Draine]

Temperatures of Interstellar Grains

- The “temperature” of a dust grain is a measure of the internal energy present in vibrational modes and possibly also in low-lying electronic excitations.
- Grain Heating
 - In diffuse regions, where ample starlight is present, grain heating is dominated by absorption of starlight photons.
 - In dense dark clouds, grain heating can be dominated by inelastic collisions with atoms or molecules from the gas (grain-grain collisions are too infrequent).
- When an optical or UV photon is absorbed by a grain, an electron is raised into an excited electronic state; three cases can occur.
 - If the electron is sufficiently energetic, it may be able to escape from the solid as a **“photoelectron.”**
 - In most solids or large molecules, however, the electronically excited state will deexcite nonradiatively, with the energy going into ***many vibrational modes - i.e., heat.***

Temperature of Large Grains and Small Grains

- Large Grains
 - Grains with radii $a \gtrsim 0.03 \mu\text{m}$, can be considered “classical.” These grains are macroscopic
 - absorption or emission of single quanta do not appreciably change the total energy in vibrational or electronic excitations.
 - The temperature of a large dust grain can be obtained by equating the heating rate to the cooling rate.
- Very Small Grains
 - For ultra-small particles, ranging down to large molecules, quantum effects are important (this include the “spinning” dust grains responsible for microwave emission).
 - When a dust particle is very small, its temperature will fluctuate. This happens because whenever an energetic photon is absorbed, the grain temperature jumps up by some not negligible amount and subsequently declines as a result of cooling.
 - To compute their emission, we need their optical and thermal properties.
 - ▶ The optical behavior depends in a sophisticated way on the the complex index of refraction and on the particle shape.
 - ▶ The thermal behavior is determined more simply from the specific heat.
 - We need to calculate the distribution function of temperature.

Heating & Cooling

- Radiative Heating rate (for a single particle):
 - the rate of heating of the grain by absorption of radiation can be written.

$$\begin{aligned} \left(\frac{dE}{dt} \right)_{\text{abs}} &= \int \frac{u_\nu d\nu}{h\nu} \times c \times h\nu \times Q_{\text{abs}}(\nu) \pi a^2 \\ &= \int d\nu 4\pi J_\nu Q_{\text{abs}}(\nu) \pi a^2 \end{aligned}$$

Here, $u_\nu d\nu/h\nu$ is the number density of photons; the photons move at the speed of light c and carry energy $h\nu$.

- Radiative Cooling rate (for a single particle)

- Kirchhoff's Law in LTE

j_ν = emissivity per unit volume

κ_ν = absorption coefficient per unit length

j_ν/n_d = emissivity per particle

$\kappa_\nu/n_d = C_{\text{abs}}(\nu)$ = absorption cross section

n_d = number density of dust particles

$$\frac{j_\nu}{\kappa_\nu} = B_\nu(T) \Rightarrow \frac{j_\nu}{n_d} = C_{\text{abs}}(\nu) B_\nu(T)$$

[$B_\nu(T)$ = Planck function, $\kappa_\nu = n_d C_{\text{abs}}(\nu)$]

- Grains lose energy by infrared emission at a rate:

$$\left(\frac{dE}{dt} \right)_{\text{emiss}} = \int d\nu 4\pi j_\nu / n_d = \int d\nu 4\pi B_\nu(T_d) C_{\text{abs}}(\nu)$$

Equilibrium Temperature

- Steady state temperature of large grains
 - The balance equation between the heating and cooling is:

$$\left(\frac{dE}{dt} \right)_{\text{abs}} = \left(\frac{dE}{dt} \right)_{\text{emiss}} \Rightarrow \text{calculate the temperature of grains.}$$

- In general, the absorption cross section in the far-IR can be approximated as a power-law in frequency,

$$Q_{\text{abs}}(\nu) = Q_0(\nu/\nu_0)^\beta = Q_0(\lambda/\lambda_0)^{-\beta} \quad (1 \lesssim \beta \lesssim 2)$$

- As a result, the temperature of a large grain is given by:

$$T_d \approx 16.4 (a/0.1 \mu\text{m})^{-1/15} U^{1/6} \text{ K, silicate} \quad (0.01 \lesssim a \lesssim 1 \mu\text{m})$$

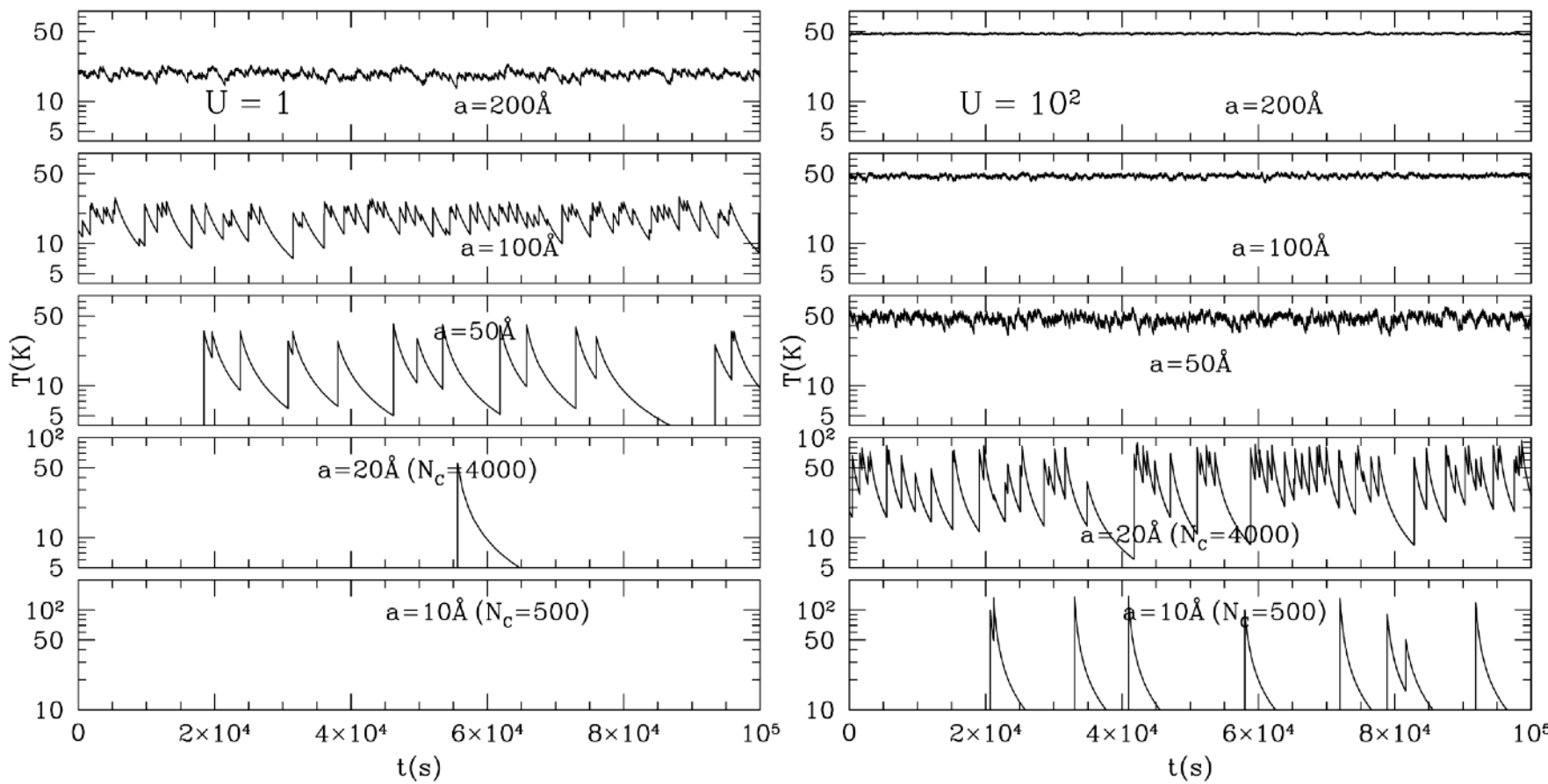
$$\approx 22.3 (a/0.1 \mu\text{m})^{-1/40} U^{1/6} \text{ K, graphite} \quad (0.005 \lesssim a \lesssim 0.15 \mu\text{m})$$

U = strength of the interstellar radiation field in units of Mathis model.

- Implications
 - ▶ If the ISRF is doubled, the grain temperature increases by $\sim 12\%$. In order to increase the temperature by a factor of 2, 64 times stronger radiation is required.
 - ▶ ***There is also little dependence of the grain temperature on grain radius. Therefore, large grains can be regarded to be grains with a single size.***

Stochastic Heating of Very Small Grains

- Temperature History:
 - ▶ Two effects become increasingly important with diminishing grain size: (1) the heat capacity of the dust becomes sufficiently small that single-particle hits can cause large spikes in the dust temperature and (2) the absorption rate with photons becomes sufficiently low that the cooling of the dust between successive collisions becomes important.
 - ▶ ***Therefore, for very small dust grains, it is clear that one cannot speak of a representative grain temperature under these conditions - one must instead use a temperature distribution function.***



Monte-Carlo simulations of the temperature fluctuation: Temperature versus time during 10^5 s (~ 1 day) for five carbonaceous grains in two radiation fields: the local starlight intensity ($U = 1$; left panel) and 10^2 times the local starlight intensity ($U = 10^2$; right panel). The importance of quantized stochastic heating is evident for the smallest sizes.

[Fig 24.5, Draine]

Formation of Stars

Star-Gas-Star Cycle

- Stars (and their planetary systems) are formed out of the ISM material through gravitational contraction, making for a kind of star-gas-star cycle.

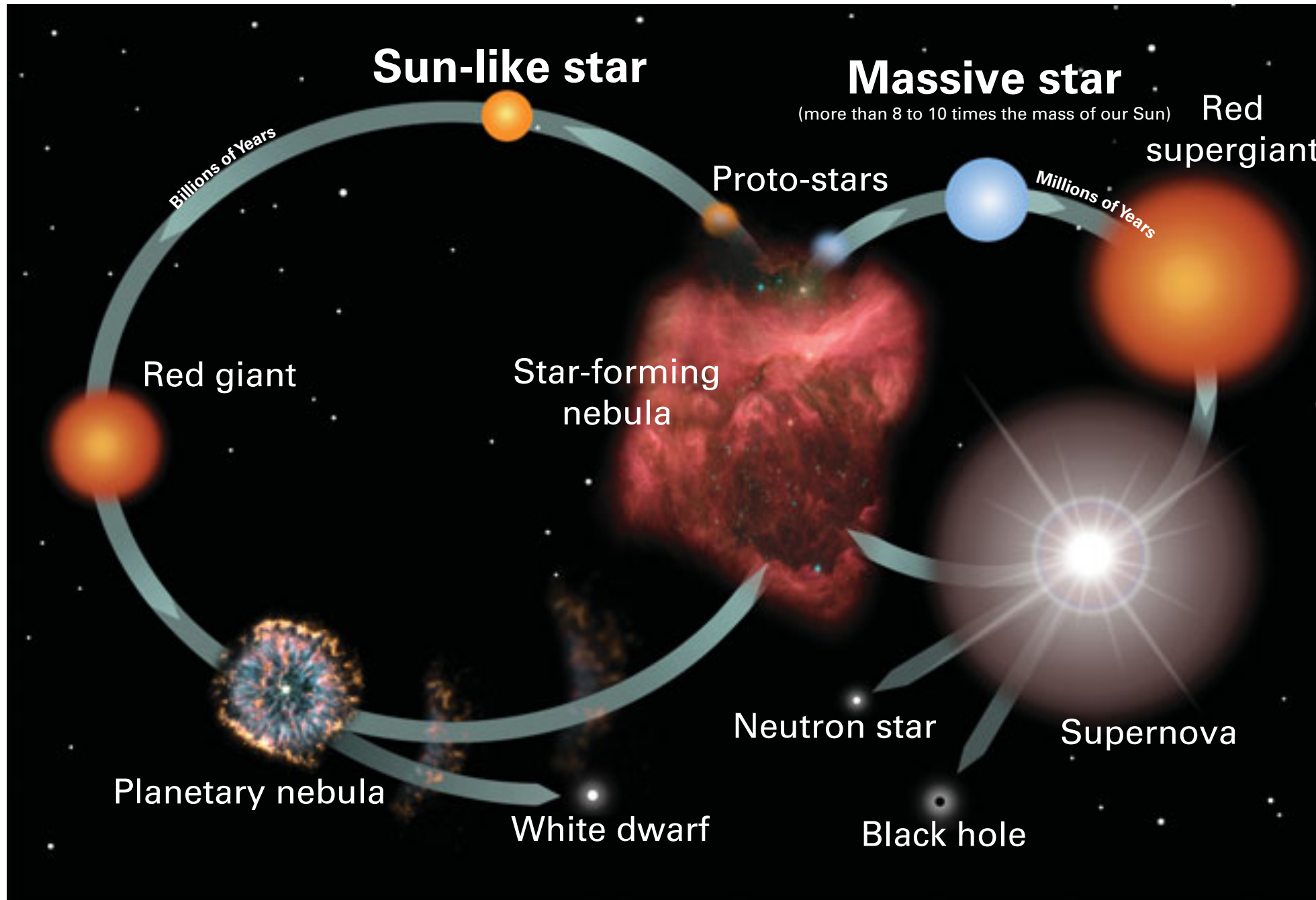


Illustration of formation of solar-type and massive stars from interstellar cloud [S. Owocki]

Star-Gas Cycle

- Assume that, on average, ***a typical atom spends roughly equal fractions of time in the star versus the ISM phase of this cycle,***
 - then the average density of gas in the ISM should be roughly equal to the mass of the stars spread out over the volume between them.
 - In the region of the Galaxy near the Sun (solar neighborhood), a typical separation between stars is

$$d \approx 2 \text{ pc}$$

- the mean number density of stars

$$n_* \approx 1/d^3 \approx 0.1 \text{ pc}^{-3}$$

- If we take the average mass of each star to be roughly that of the Sun, we obtain a mean mass density

$$\rho \approx M_\odot n_* \approx 7 \times 10^{-24} \text{ g/cm}^3$$

- With a composition dominated by hydrogen, the associated ISM hydrogen-atom number density is

$$n \approx \rho/m_p \approx 4 \text{ cm}^{-3}$$

- The characteristic ISM number $n \approx 1 \text{ cm}^{-3}$ is comparable to this “very rough” estimate.

Virial Theorem

- The virial theorem is a relation between the total kinetic energy and the total potential energy of a stable bound systems, .i.e., systems that hang together forever and whose parameters (such as velocities and coordinates of the particles) are finite.
 - The virial theorem provides a general equation that relates **the average over time of the total kinetic energy** of a stable, self-gravitating system of discrete particles, with **the total potential energy** of the system.

$$2 \langle K \rangle + \langle U \rangle = 0$$

- The virial theorem has a wide range of applications in astrophysics, from the formation of stars (in which case the bodies of the system are the atoms of the gas) to the formation of the largest structures in the universe, the clusters of galaxies.
- <https://www.uio.no/studier/emner/matnat/astro/nedlagte-emner/AST1100/h09/undervisningsmateriale/lecture5.pdf>

Jeans Criterion for Gravitational Contraction

- Stars generally form in clusters from the gravitational contraction of a dense, cold GMC.
 - The requirements for such gravitational contraction depend on the relative magnitudes of the total internal thermal (kinetic) energy K versus the gravitational binding energy U .
 - For a cloud of mass M , uniform temperature T , and mean mass per particle μ , the total number of particles $N = M/\mu$ have an associated total thermal energy,

$$K = \frac{3}{2} N k_B T = \frac{3}{2} \frac{M k_B T}{\mu}$$

- For a spherical cloud with radius R and uniform density, the associated gravitational binding energy is

$$U = -\frac{3}{5} \frac{GM^2}{R}$$

- Recall that $K = -U/2$ is the condition for stably bound systems in virial equilibrium.
- Therefore, for a cloud with $K > -U/2$, the excess internal pressure would do work to expand the cloud against gravity, leading to it to be unbound.
- Conversely, for $K < -U/2$, the too-low pressure would allow the cloud to gravitationally contract, leading to a more strongly bound cloud.

- The critical requirement, known as the ***Jeans criterion***, for gravitational contraction can be obtained from the above argument.

$$K < -U/2 \implies \frac{3}{2} \frac{Mk_B T}{\mu} < \frac{3}{10} \frac{GM^2}{R} \implies \frac{M}{R} > \frac{5k_B T}{G\mu}$$

- ***Jeans radius*** (in terms of the number density of atom $n = \rho/\mu$)

$$M = \frac{4\pi}{3} R^3 n \mu \implies R > \left(\frac{15}{4\pi} \frac{k_B T}{G n \mu^2} \right)^{1/2} \equiv R_J$$

molecular hydrogen
↓

$$R_J \approx 15 \text{ pc} \left(\frac{T/100 \text{ K}}{n/10 \text{ cm}^{-3}} \right)^{1/2} \left(\frac{2m_p}{\mu} \right)$$

- ***Jeans mass***

$$M > \frac{4\pi}{3} R_J^3 n \mu = \frac{5}{\mu^2} \left(\frac{15}{4\pi n} \right)^{1/2} \left(\frac{k_B T}{G} \right)^{3/2} \equiv M_J$$

$$M_J \approx 7300 M_{\odot} \frac{(T/100 \text{ K})^{3/2}}{(n/10 \text{ cm}^{-3})^{1/2}} \left(\frac{2m_p}{\mu} \right)^2$$

- For typical ISM conditions, both the Jeans radius and mass are quite large, implying it can be actually quite difficult to initiate gravitational contraction.
- A general conclusion of such a large Jeans mass is that **stars tend typically to be formed in large clusters, resulting from an initial contraction of a GMC**, with mass of order 10^4 solar mass or more.
- ***Jeans fragmentation***: The Jeans length and mass both scale inversely with the square root of the density. This suggests that **a collapsing cloud may break into multiple smaller pieces** as it becomes denser.

Free-fall time (Dynamical time scale)

- **Free-fall timescale**

- In the absence of any support, the collapse can be described as a free-fall with acceleration determined by the gravitational force,

$$m \frac{d^2r}{dt^2} = -\frac{GMm}{r^2} \quad (m = \text{test particle mass})$$

- boundary condition: $v = \frac{dr}{dt} = 0$ at the outer radius $r = R$

$$\frac{d^2r}{dt^2} = \frac{dv}{dr} \frac{dr}{dt} = \frac{1}{2} \frac{dv^2}{dr} \longrightarrow \frac{dv^2}{dr} = -\frac{GM}{r^2} \implies v^2 = 2GM \left(\frac{1}{r} - \frac{1}{R} \right) \implies \frac{dr}{dt} = -\left[2GM \left(\frac{1}{r} - \frac{1}{R} \right) \right]^{1/2}$$

$$\int_0^{t_{ff}} dt = - \int_R^0 \frac{dr}{\left[2GM \left(\frac{1}{R} - \frac{1}{r} \right) \right]^{1/2}} = \left(\frac{2R^3}{GM} \right)^{1/2} \frac{\pi}{4}$$

the negative sign is chosen because the core is collapsing.

- free-fall time (the times for the test particle to move from the outer radius to the center)

$$M = \frac{4}{3}\pi R^3 \rho \rightarrow t_{ff} = \left(\frac{3\pi}{32G\rho} \right)^{1/2} = 3.6 \left(\frac{100 \text{ cm}^{-3}}{n} \right)^{1/2} \left(\frac{2m_p}{\mu} \right)^{1/2} \text{ Myr}$$

- Note that we assumed no force against the gravity. But, there will be a significant source of internal pressure against the gravity while the material collapse.

• Star Formation Efficiency

- In our Galaxy, the total mass in GMCs with density $n \gtrsim 100 \text{ cm}^{-3}$ is $M_{\text{GMC}} \approx 10^9 M_{\odot}$. Since this mass should collapse to stars over a free-fall time, it suggests an overall galactic star-formation rate is given by

$$\dot{M}_{\text{SFR}} = \frac{M_{\text{GMC}}}{t_{\text{ff}}} \approx 280 M_{\odot} \text{ yr}^{-1}$$

- But the observationally inferred star-formation rate is much smaller, only $\sim 1 M_{\odot} \text{ yr}^{-1}$, implying an star-formation efficiency of only

$$\epsilon_{\text{ff}} \lesssim 0.01$$

**star formation efficiency =
the mass fraction of a cloud that ultimately turns into stars in a unit time interval**

- The reasons for this are not entirely clear, but may stem in part from inhibition of gravitational collapse by **interstellar magnetic fields**, and/or by **interstellar turbulence**.
- Another likely factor is the **feedback from hot, massive stars**, which heat up and ionize the cloud out of which they form, thus preventing the further gravitational contraction of the cloud into more stars.
- Modeling this feedback loop is a major challenge and a topic of current research.

Fragmentation into Cold Cores

- **Fragmentation**

- In those portions of a GMC that do undergo gravitational collapse, the contraction soon leads to higher densities, and thus to smaller Jeans mass and Jeans radius, along with a shorter free-fall time.

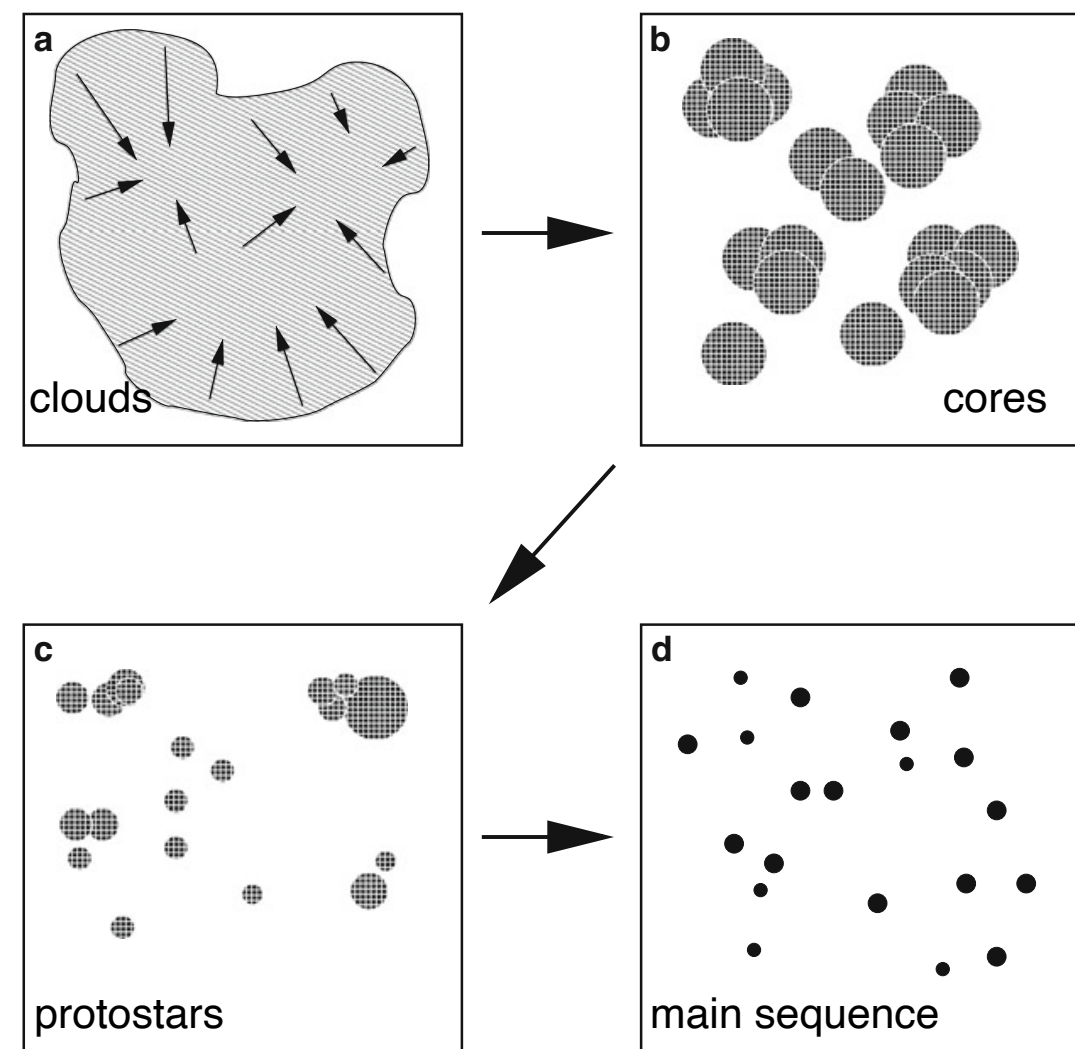
because $M_J \propto \rho^{-1/2}$, $R_J \propto \rho^{-1/2}$, and $t_{\text{ff}} \propto \rho^{-1/2}$

- This tends to cause the overall cloud, with total mass, to fragment into much smaller, stellar-mass cloud “cores” that will form into individual stars.

- The fragmentation process is a hierarchical process in which parent clouds break up into subclouds, which may themselves break into smaller structures.

- ◆ 10 kpc - spiral arms of the Galaxy
- ◆ 1 kpc - H I super clouds
- ◆ 100 pc - giant molecular clouds
- ◆ 10 pc - molecular clouds
- ◆ 0.1 pc - molecular cloud cores
- ◆ 100 AU - protostars

- Stars are the final step of fragmentation.



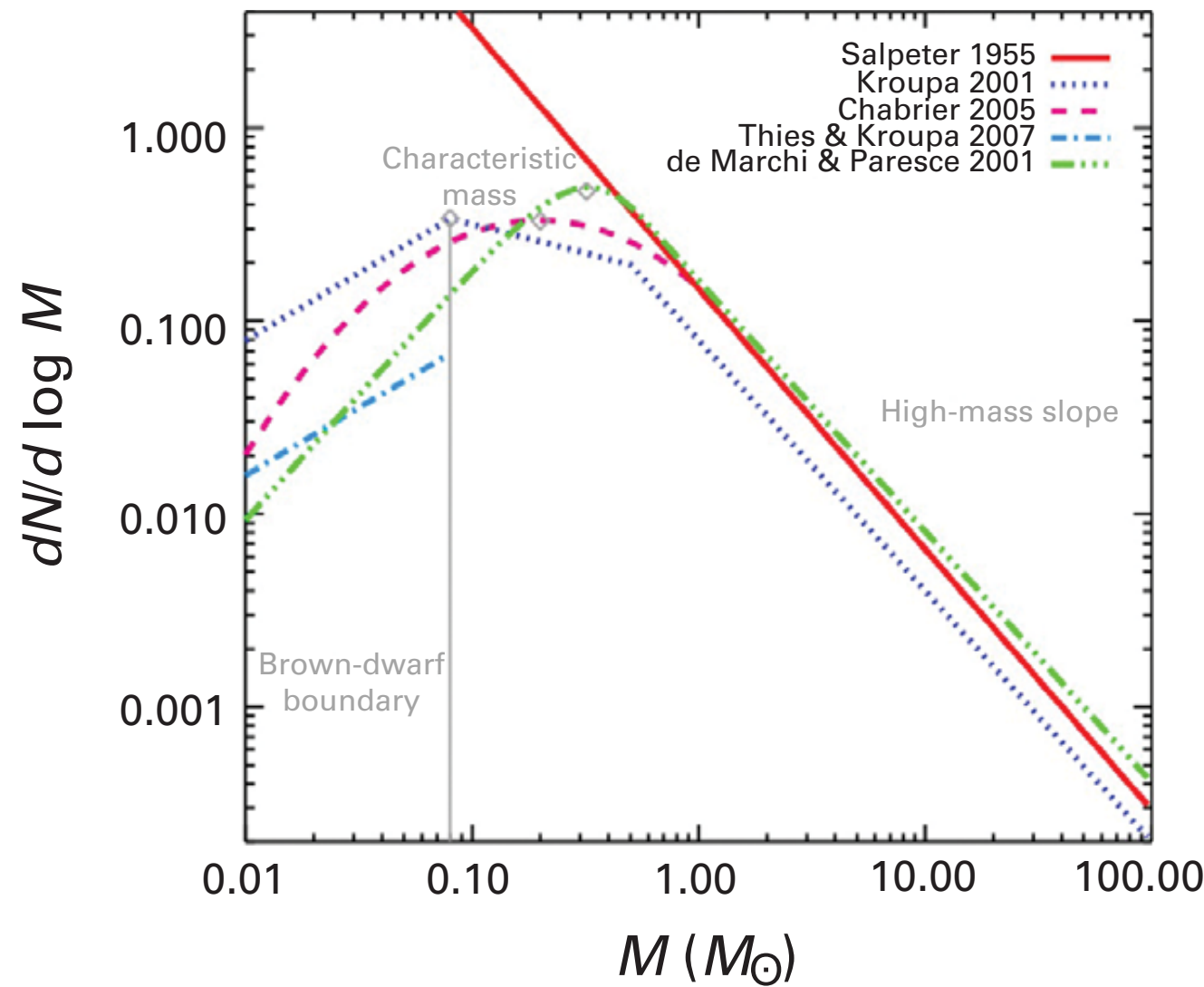
Initial Mass Function

- Initial Mass Function
 - A key, still-unsolved issue in star formation regards the physical processes and conditions that determine the mass distribution of these proto-stellar cores, leading then to what is known as the stellar initial mass function (IMF).
 - ***IMF = the number of stars per a unit mass range as a function of mass.***
 - Studies of the evolution of stellar clusters suggest that this can be roughly characterized by a power-law form:

$$\frac{dN}{dm} = K m^{-\alpha} \quad (\alpha \approx 2.35 \text{ for } m > 1 M_{\odot}; \text{ Salpeter IMF})$$

- Here, K is a normalization factor that depends on the total number of stars. ***The large power-law index reflects the fact that higher-mass stars are much rarer than lower-mass stars.***

- More modern models generally flatten the distribution at lower-mass, as illustrated in the following figure. This allows them to be normalized to a finite number when integrated over all masses.



Comparison of IMFs from various authors.

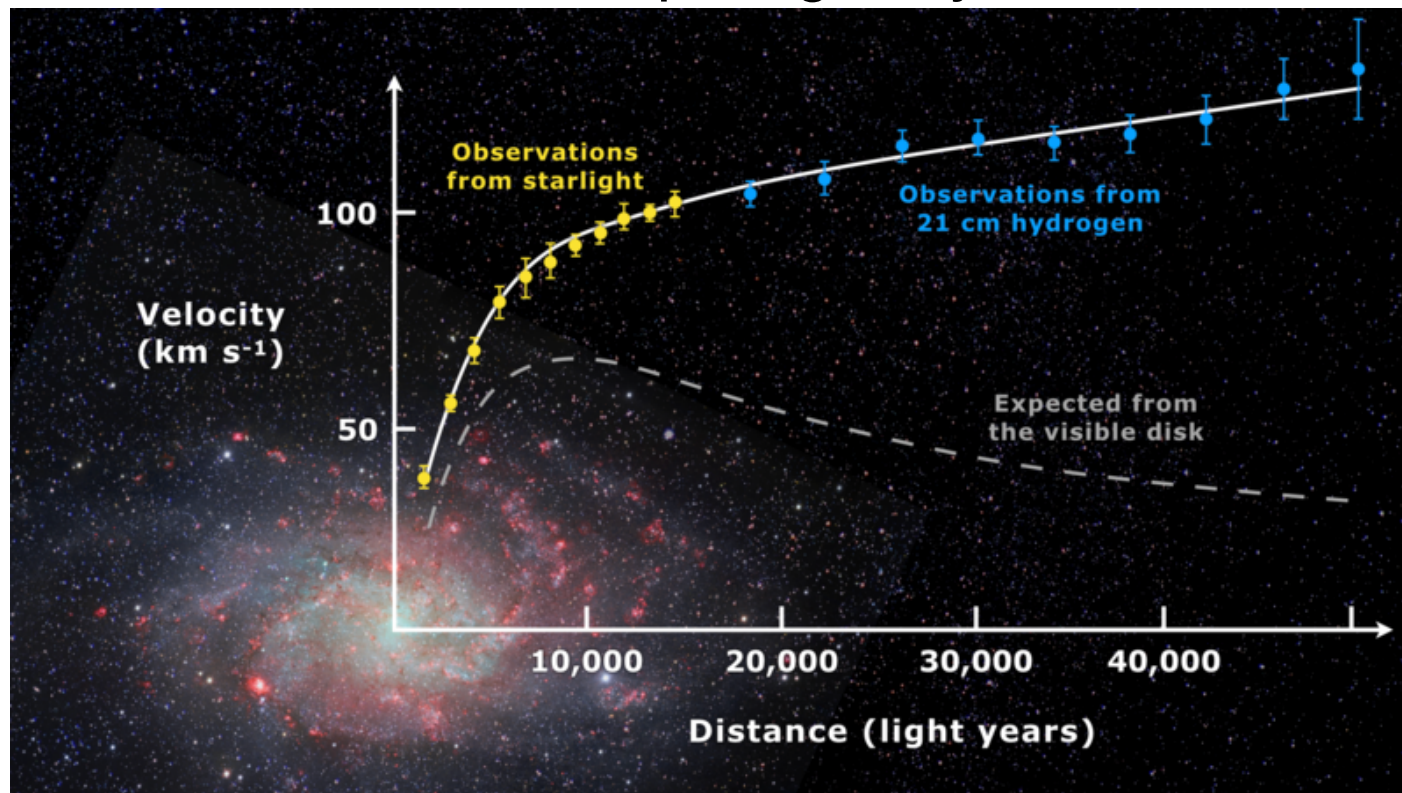
Except for the Salpeter pure-power-law form, the curves are normalized such that the integral over mass is unity.

[Offner et al. 2014]

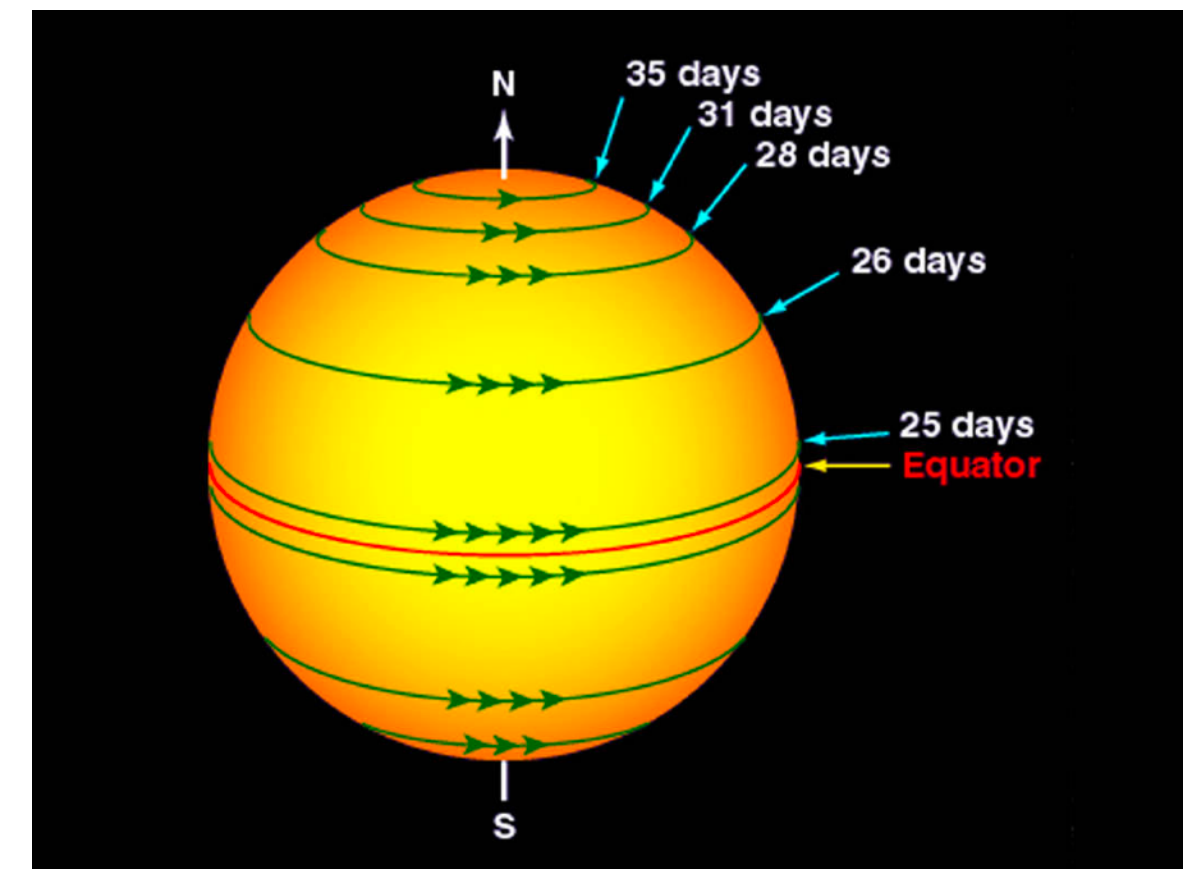
- With a given form of the IMF for a collapsing GMC, one can model the evolution of the resulting stellar cluster, based on how each star with a given mass evolves through its various evolutionary phases, e.g., main sequence, red giant, etc.

Angular Momentum: Rotation is ubiquitous

Rotation of spiral galaxy M33



Rotation of the Sun

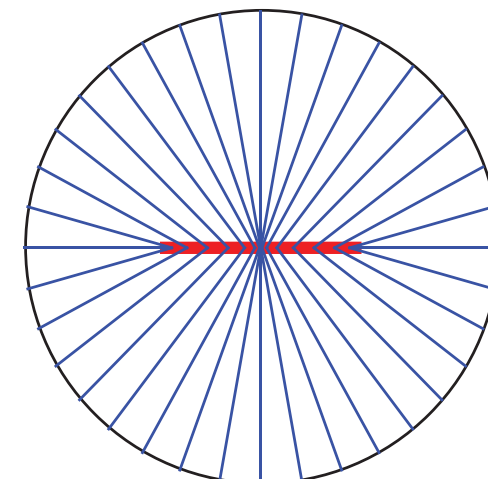


Core Collapse - Angular Momentum Conservation

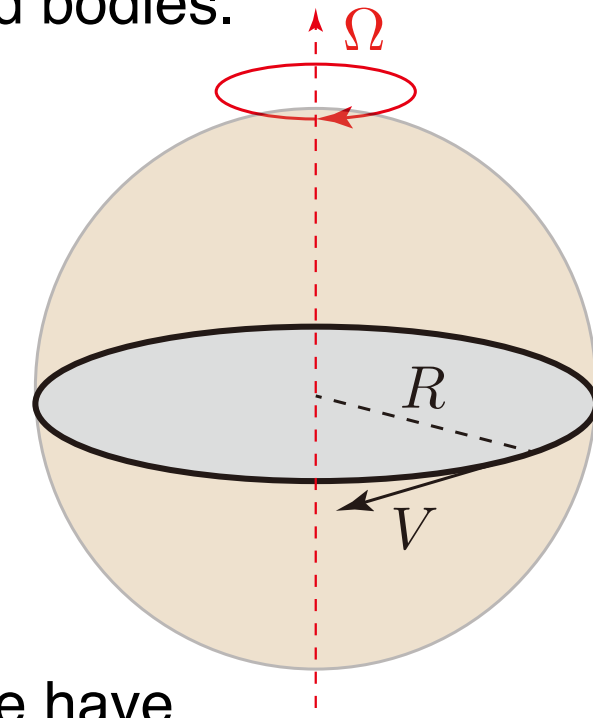
- The gravitational collapse of a cloud core to a star is accompanied by an enormous change in size scale, about six to seven orders of magnitude.

$$\frac{R_{\text{core}}}{R_{\text{star}}} \approx \frac{0.2 \text{ pc}}{3 \times 6.9 \times 10^5 \text{ km}} \approx 3 \times 10^6 \quad \leftarrow \quad \begin{array}{l} \text{Assuming} \\ R_{\text{star}} \approx 3R_{\text{sun}} \end{array}$$

- Rotation is a ubiquitous phenomenon from the largest to the smallest scales in our Galaxy; the Galaxy itself rotates as a whole, its individual stars spin too.
- In the same way as ice skaters spin faster as they pull in their arms, if all the angular momentum of the core were to be transferred to the star, it would rotate very rapidly.
- It is observed that molecular clouds do have a small amount of rotation, with velocities of order ***a few hundred meters per second*** ($\sim 0.15 \text{ km/s}$).
- ***The formation of “planets” around stars would not be possible if a certain amount of angular momentum was not present at the beginning of the star formation process.*** The angular momentum thus plays a significant role during the process of star and planet formation.



- Consider the gravitational collapse of a uniform spherical core with radius R_{core} and mass M to a star with radius R_{star} . We will assume that they are rigid bodies.



rotational speed (angular frequency): $\Omega = V/R$

moment of inertia: $I = (2/5)MR^2$

angular momentum: $J = I\Omega$

rotation period: $P = 2\pi/\Omega = 2\pi R/V$

- From the conservation of “mass” and “angular momentum,” we have

$$I_{\text{core}}\Omega_{\text{core}} = I_{\text{star}}\Omega_{\text{star}} \implies MR_{\text{core}}^2\Omega_{\text{core}} = MR_{\text{star}}^2\Omega_{\text{star}} \longrightarrow$$

$$\therefore \Omega_{\text{star}} = \left(\frac{R_{\text{core}}}{R_{\text{star}}}\right)^2 \Omega_{\text{core}}$$

$$P_{\text{star}} = \left(\frac{R_{\text{star}}}{R_{\text{core}}}\right)^2 P_{\text{core}}$$

For $R_{\text{core}} = 0.2 \text{ pc}$,

$R_{\text{star}} = 3R_{\odot} = 3 \times (7 \times 10^8) \text{ m}$,

$V_{\text{core}} = 150 \text{ m s}^{-1}$

We obtain $P_{\text{star}} \simeq 10^{-13} P_{\text{core}}$, $P_{\text{core}} \simeq 0.9 \text{ Myr}$, $P_{\text{star}} \simeq 0.5 \text{ mins}$

$P_{\text{sun}} \simeq 27 \text{ days}$ for reference

- **Stars cannot spin that fast because they would tear apart.** Instead, the core may fragment as its density increases and form more than one star. The bulk of the core rotation then goes into orbital motion of multiple stars (and/or planets) rather than the rotation of a single star.

Core Collapse - Disk Formation

- Ultimately, a core that collapses to a single object will contract until gravity is balanced by centrifugal force. This only acts perpendicular to the rotational axis so the spherical core flattens to a disk.
- If we consider a test particle with mass m at radius R rotating at speed V , the ratio of the two forces is

$$\frac{F_{\text{grav}}}{F_{\text{cen}}} = \frac{GMm/R^2}{mv^2/R} = \frac{GM}{R^3\Omega^2}$$

The condition of $F_{\text{grav}} = F_{\text{cen}}$ is called “Keplerian motion.”

- At the **outer boundary of the disk**, this ratio should be equal to 1.

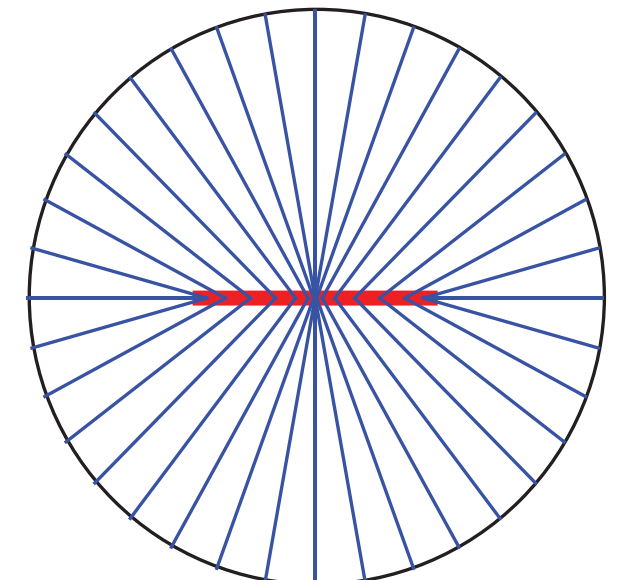
$$R_{\text{disk}}^3\Omega_{\text{disk}}^2 = GM \quad \text{Eq (a)}$$

- Assuming the conservation of angular momentum,

$$R_{\text{disk}}^2\Omega_{\text{disk}} = R_{\text{core}}^2\Omega_{\text{core}} \implies R_{\text{disk}}^4\Omega_{\text{disk}}^2 = R_{\text{core}}^4\Omega_{\text{core}}^2 \quad \text{Eq (b)}$$

- Therefore, after dividing Eq (b) by Eq (a), we have

$$R_{\text{disk}} = \frac{R_{\text{core}}^4\Omega_{\text{core}}^2}{GM} = 2\beta_{\text{eq}}R_{\text{core}} \iff \beta_{\text{eq}} \equiv \frac{\Omega_{\text{core}}^2 R_{\text{core}}^2 / 2}{GM/R_{\text{core}}}$$



Core Collapse - Disk Formation

- Here, β is ***the ratio of rotational to gravitational energy*** at the equator of the core.

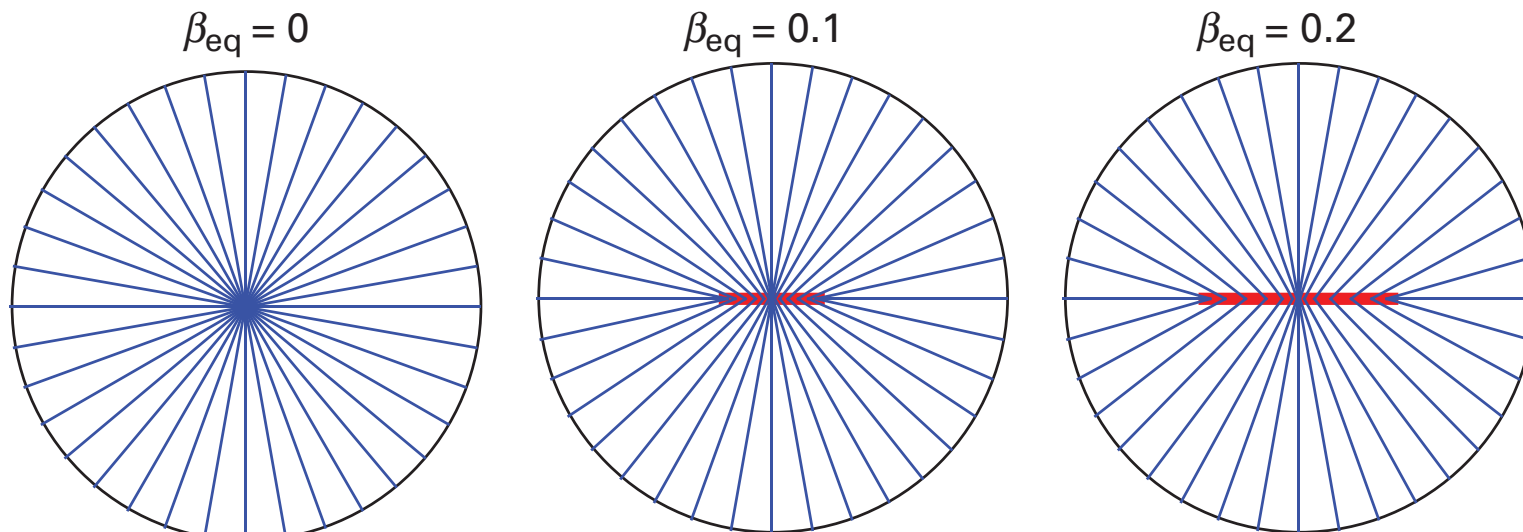
$$\beta_{\text{eq}} \equiv \frac{\Omega_{\text{core}}^2 R_{\text{core}}^2 / 2}{GM/R_{\text{core}}}$$

- Observations of cloud cores gives a typical value of $\beta_{\text{eq}} \approx 0.02$ (Goodman et al. 1993).
- For a cloud core size $R \approx 0.05$ pc, the expected disk radius is a few hundred AU, comparable to the inferred sized of proto-stellar disks.

$$R_{\text{disk}} \approx 410 \text{ AU} \left(\frac{\beta_{\text{eq}}}{0.02} \right) \left(\frac{R_{\text{core}}}{0.05 \text{ pc}} \right)$$

$R_{\text{heliosphere}} \approx 100 \text{ AU}$ for reference

- The following figure illustrates, for various values of β_{eq} , how material from various latitudes in the original clouds track toward the center star or disk under gravitational collapse.



black circle: rigidly rotating spherical cloud
red: orbiting disk

- In disks with Keplerian orbits, the orbital frequency increase inward with radius $\Omega \sim r^{-3/2}$, meaning that between two neighboring rings there is an overall shear in orbital speed.
 - ◆ Any frictional interaction - due to viscosity - between such neighboring rings will tend to transport angular momentum from the faster inner ring to the slower outer ring, allowing the inner mass to fall further inward, while the angular momentum receiving material moves further outward.
 - ◆ This outward viscous diffusion of angular momentum allows, over time, for most of the mass to accrete onto the star, with just a small mass fraction retaining the original angular momentum.
- Eventually, this remnant disk-mass can fragment into its own gravitationally collapsing cores to form planets.
 - ◆ In our solar system, the most massive planet Jupiter has only 0.1% the mass of the Sun, but 99% of the solar system's angular momentum.
 - ◆ Earth too originated from the evolving proto-solar disk.

Young Stellar Objects (YSOs)

- Young Stellar Object denotes a star in its early stage of evolution.
 - ◆ This class consists of two groups of objects: protostars and pre-main-sequence stars.
 - ◆ A **protostar** is a very young star that is still gathering mass from its parent molecular cloud.
 - ▶ A dense core is initially in balance between self-gravity and gas/magnetic pressure. As the dense core acquires mass from its larger, surrounding cloud, self-gravity begins to overwhelm pressure, and collapse begins. The protostellar phase begins when the molecular cloud fragment first collapses under the force of self-gravity and an opaque, pressure supported core forms inside the collapsing fragment.
 - ▶ The gas that collapses toward the center of the dense core first builds up a low-mass protostar, and then a protoplanetary disk orbiting the object. As the collapse continues, an increasing amount of gas impacts the disk rather than the star, a consequence of angular momentum conservation.
 - ◆ The protostellar phase ends when the infalling gas is depleted, leaving a **pre-main-sequence star**.
 - ▶ **After the protostar blows away the envelope, it is optically visible, and appears on the Hayashi track** in the Hertzsprung-Russell diagram. A pre-main-sequence star contracts to later become a main-sequence star at the onset of hydrogen fusion producing helium.
 - ▶ **The energy source of PMS objects is gravitational contraction**, as opposed to hydrogen burning in main-sequence stars.

• **Protostar**

- **Maximum infall rate:** Combining the free-fall timescale and maximum stable core mass, we can derive an upper limit to the mass infall rate.

$$\dot{M}_{\text{in}} = \frac{M_{\text{BE}}}{t_{\text{ff}}} \approx 2.2 \frac{c_s^3}{G}$$

$$\approx 4 \times 10^{-6} M_\odot/\text{yr}$$

←

$$M_{\text{BE}} = 1.5 \left(\frac{2}{\pi G^3 \rho} \right)^{1/2} c_s^3$$

$$t_{\text{ff}} = \left(\frac{3\pi}{32G\rho} \right)^{1/2}$$

- **Accretion luminosity:** This is high enough that the release of gravitational energy, as gas falls from core to stellar scales, provides significant accretion luminosity.

$$L_{\text{acc}} = -GM\dot{M}_{\text{in}} \left(\frac{1}{R_{\text{core}}} - \frac{1}{R_*} \right)$$

$$\approx 9.3 \left(\frac{M}{1 M_\odot} \right) \left(\frac{\dot{M}_{\text{in}}}{10^{-6} M_\odot \text{ yr}^{-1}} \right) \left(\frac{R_*}{3R_\odot} \right)^{-1} L_\odot$$

← core radius $R_{\text{core}} \gg$ stellar radius R_*
typical size of solar-mass stars at early
times $R_* \approx 3R_\odot$

- This calculation shows that **a protostar is detectable well before it begins nuclear fusion.**
- Due to the high dust extinction of the surrounding core, the very earliest phase of star formation is only visible at $\lambda > 100 \mu\text{m}$.

- But, within $\sim 10^5$ yr after collapse, protostars become detectable in the near-IR and mid-IR.
- As the core is used up, both the dust emission and extinction decrease. The protostar becomes increasingly visible at shorter wavelengths and the longer wavelength emission decreases.
- The evolutionary state of a protostar is generally classified based on its IR SED, but mm wavelength imaging of its surrounding envelope and disk is increasingly used in addition (e.g., ALMA).

- **Pre-main sequence star**

- Once the collapse phase ends and the protostar had reached its final mass, it is known as a pre-main sequence star.
- It slowly contracts through the loss of gravitational energy by radiation on a **Kelvin-Helmholtz timescale (thermal timescale)**, which determines how quickly a star contracts before nuclear fusion starts - i.e. sets roughly the pre-main sequence lifetime

$$t_{\text{KH}} = \frac{U}{L_*} = \frac{GM_*^2/R_*}{L_*} \simeq 31.1 \left(\frac{M_*}{M_\odot} \right)^2 \left(\frac{R_*}{R_\odot} \right)^{-1} \left(\frac{L_*}{L_\odot} \right)^{-1} \text{Myr}$$

Here, U = internal thermal energy from the Virial theorem

- Pre-main sequence stars with $0.1 M_\odot < M_* < 2 M_\odot$ is known as **T Tauri stars**. These stars were first known in the 1940s and this name remains a common alternative name for pre-main sequence stars for historical reasons
- The intermediate mass counterpart, $2 M_\odot < M_* < 8 M_\odot$, are known as **Herbig Ae/Be stars**, where A and B refer to the stellar spectral types. The “e” denotes the photospheric emission lines that were used to identify their youth.
- More massive stars are much more luminous and they contract too quickly. Hence, they have no pre-main-sequence stage. By the time they become visible, the hydrogen in their centers is already fusing and they are main-sequence objects.

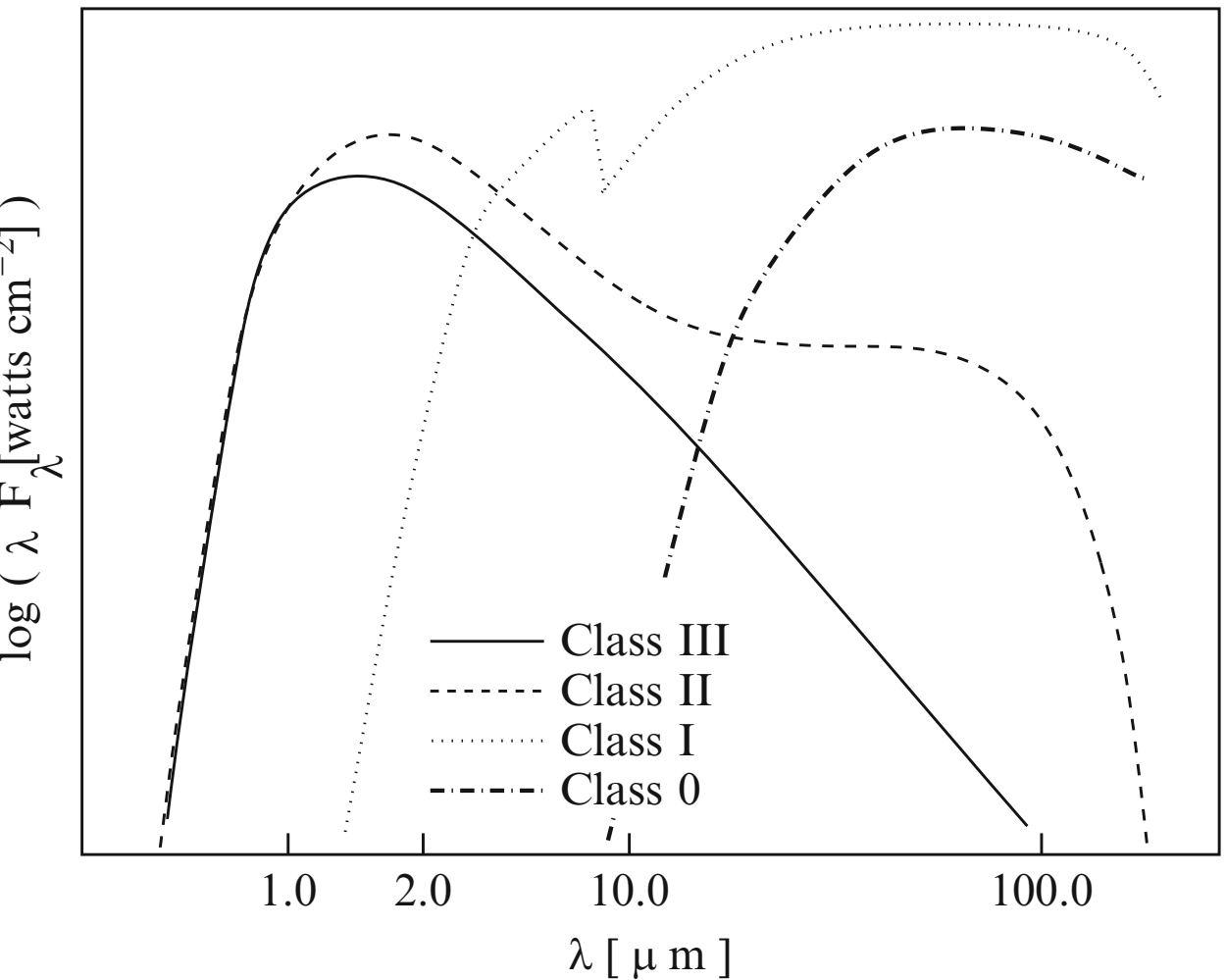
-
- Timescales in stellar evolution
 - Free-fall timescale = dynamic timescale
 - Kelvin-Helmholtz timescale = thermal timescale
 - Nuclear time scale
 - ◆ Time scale on which the star will exhaust its supply of nuclear fuel if it keeps burning it at the current rate
 - ◆ Energy release from fusing one gram of H to He is 6×10^{18} erg. Therefore, the nuclear timescale is

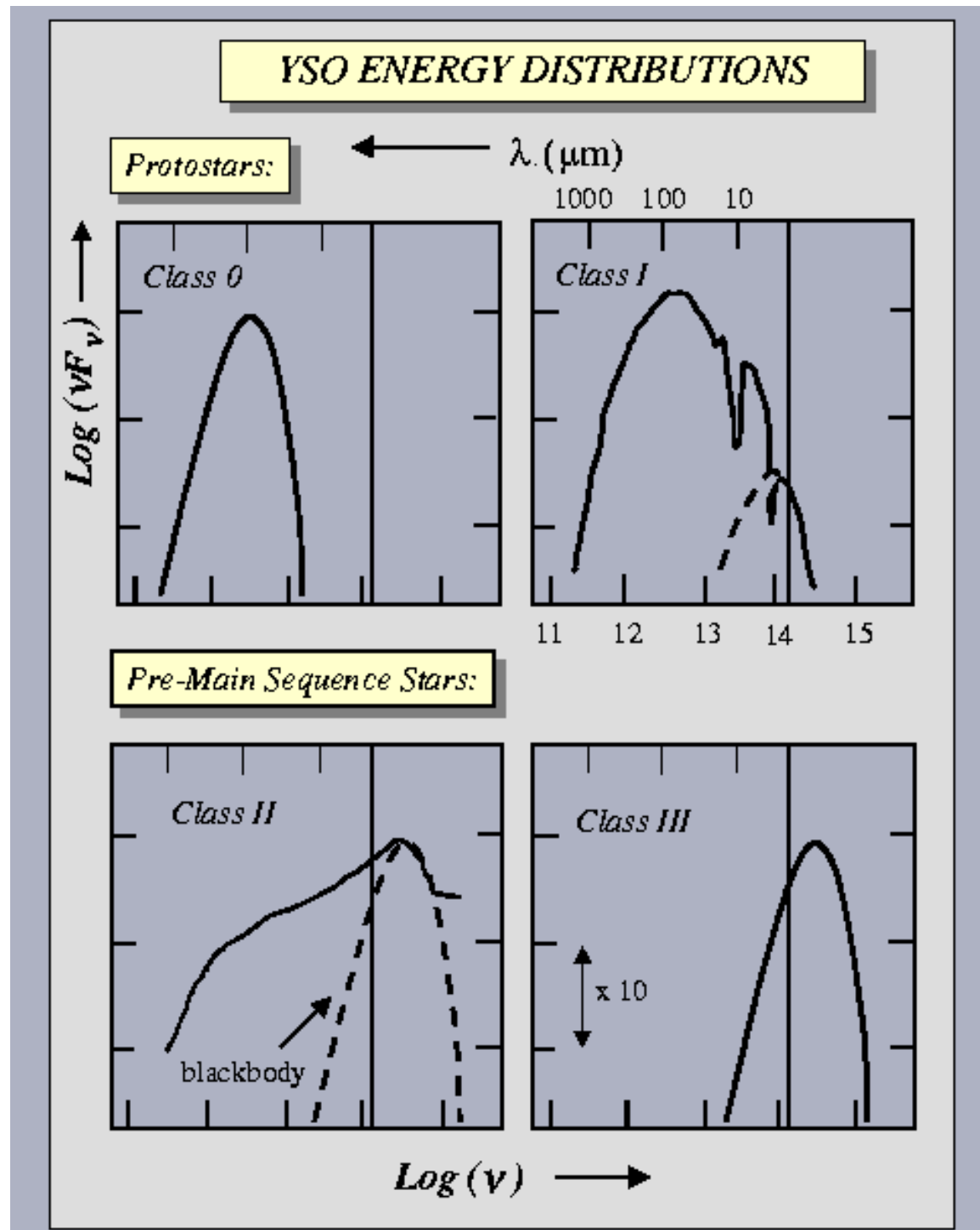
$$\begin{aligned} t_{\text{nuc}} &= \frac{q X M \times (6 \times 10^{18} \text{ erg g}^{-1})}{L_*} \\ &\approx 7 \left(\frac{X}{0.7} \right) \left(\frac{q}{0.1} \right) \left(\frac{M}{M_\odot} \right) \left(\frac{L_\odot}{L_*} \right) \text{ Gyr} \end{aligned}$$

Here, X is the mass fraction of H initially present and q is the fraction of fuel available to burn in the core.

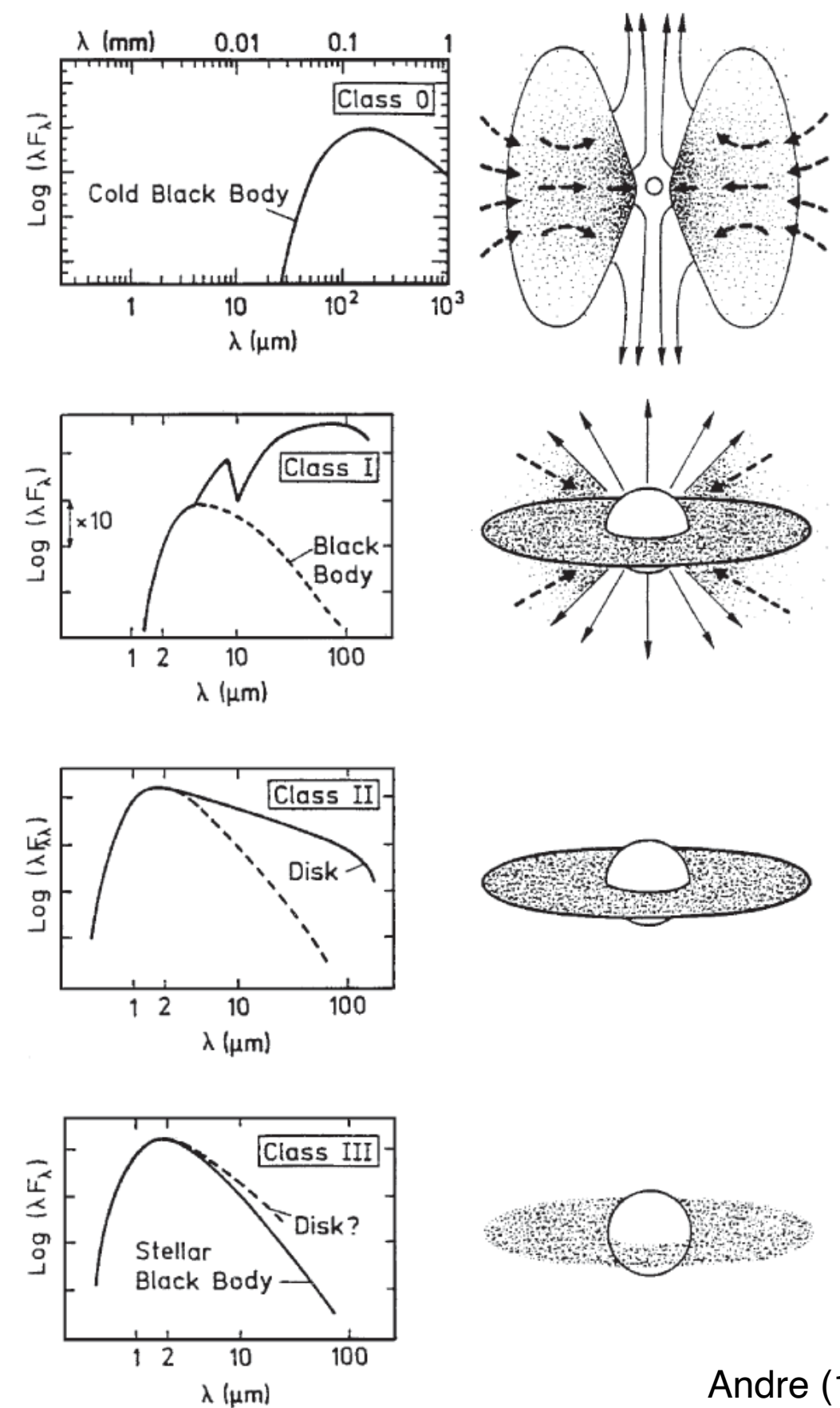
Spectral Energy Distributions (SEDs) of YSOs

- Lada & Wilking (1984) and Lada (1987) investigated SEDs of IR sources observed in the $1\text{-}100 \mu\text{m}$ wavelength band in the core of the Ophiuchi dark cloud, and proposed a general IR classification scheme.
 - ◆ A spectral index is defined between 2.2 and $25 \mu\text{m}$:
$$\alpha_{\text{IR}} = \frac{d \log(\lambda F_\lambda)}{d \log \lambda} \quad \lambda F_\lambda \propto \lambda^\alpha$$
 - ◆ Class I sources have very broad SEDs with $\alpha_{\text{IR}} > 0$.
 - ◆ Class 2 sources have $-2 < \alpha_{\text{IR}} < 0$.
 - ◆ Class 3 sources have $\alpha_{\text{IR}} < -2$.
 - ◆ The large IR excesses are attributed to thermal emission from dust in large circumstellar envelopes and Class I sources are likely to be evolved protostars.
- Andre et al. (1993) discovered embedded sources that remained undetected below $25 \mu\text{m}$ indicating significantly larger amounts of circumstellar material than in Class I sources and they proposed a younger Class 0 of YSOs.



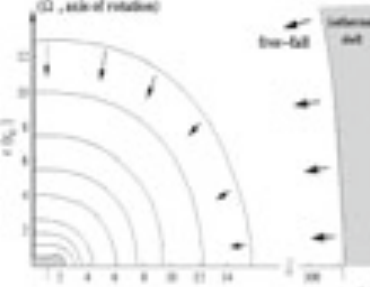
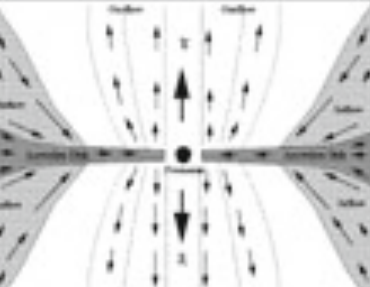
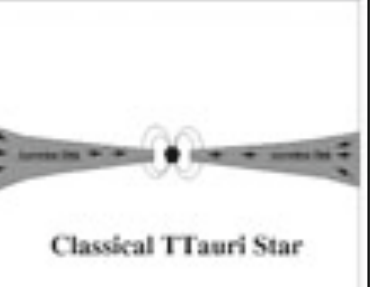
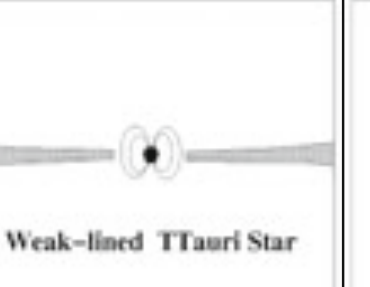


Lada (1999)



Andre (1994)

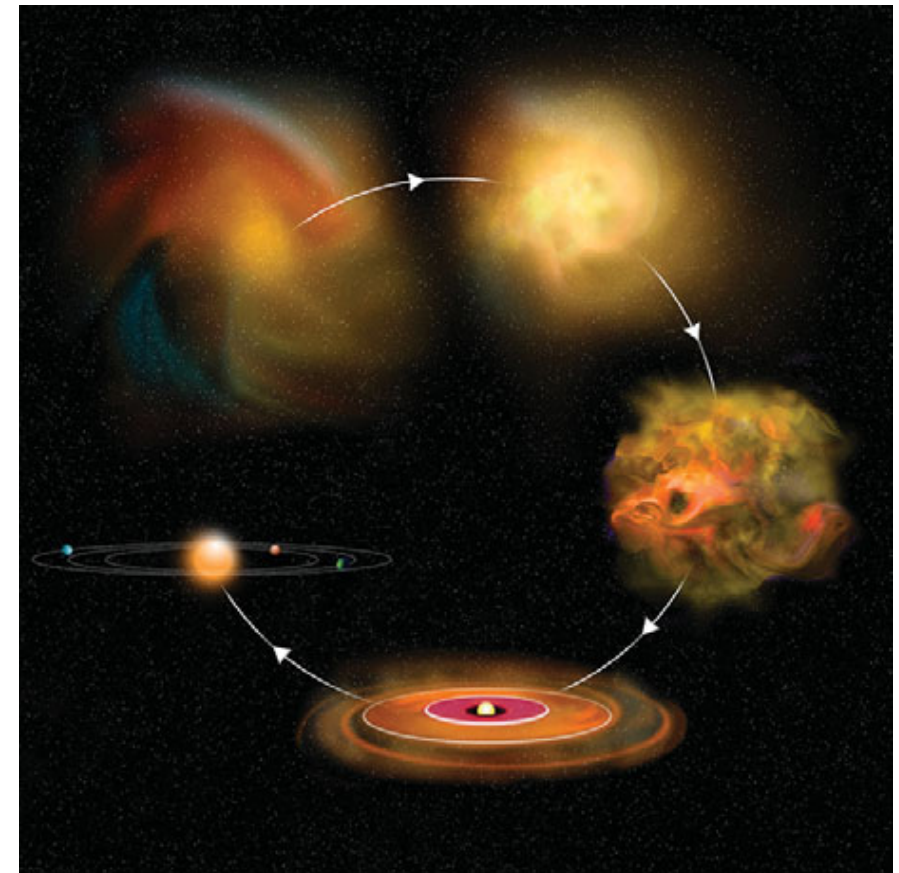
YSO classification

	Infalling protostar	Accreting protostar	Contracting PMS star	MS star
YSO properties			 Classical TTauri Star	 Weak-lined TTauri Star
Phase	adiabatic (A,B,C)	accretion (D) deuterium burning onset of convection	convective radiative onset of nuclear burning	convective radiative full nuclear burning
Matter flows	mostly infall disk & outflows form	some infall mostly accretion outflows, jets	low accretion	?
Envelope/disk size	< 10000 AU	< 1000 AU	< 400 AU	~ 100 AU
Infall/accretion rate	10^{-4}	10^{-5}	$10^{-6} -- 10^{-7}$?
Age	$10^4 - 10^5$ yr	10^5 yr	$10^6 -- 10^7$ yr	$10^6 -- 10^7$ yr
Emission bands (except IR)	thermal radio X-ray?	radio X-ray	radio optical strong X-ray	non-therm. radio optical strong X-ray
Classes	Class 0	Class I	Class II	Class III
				ZAMS

Planets

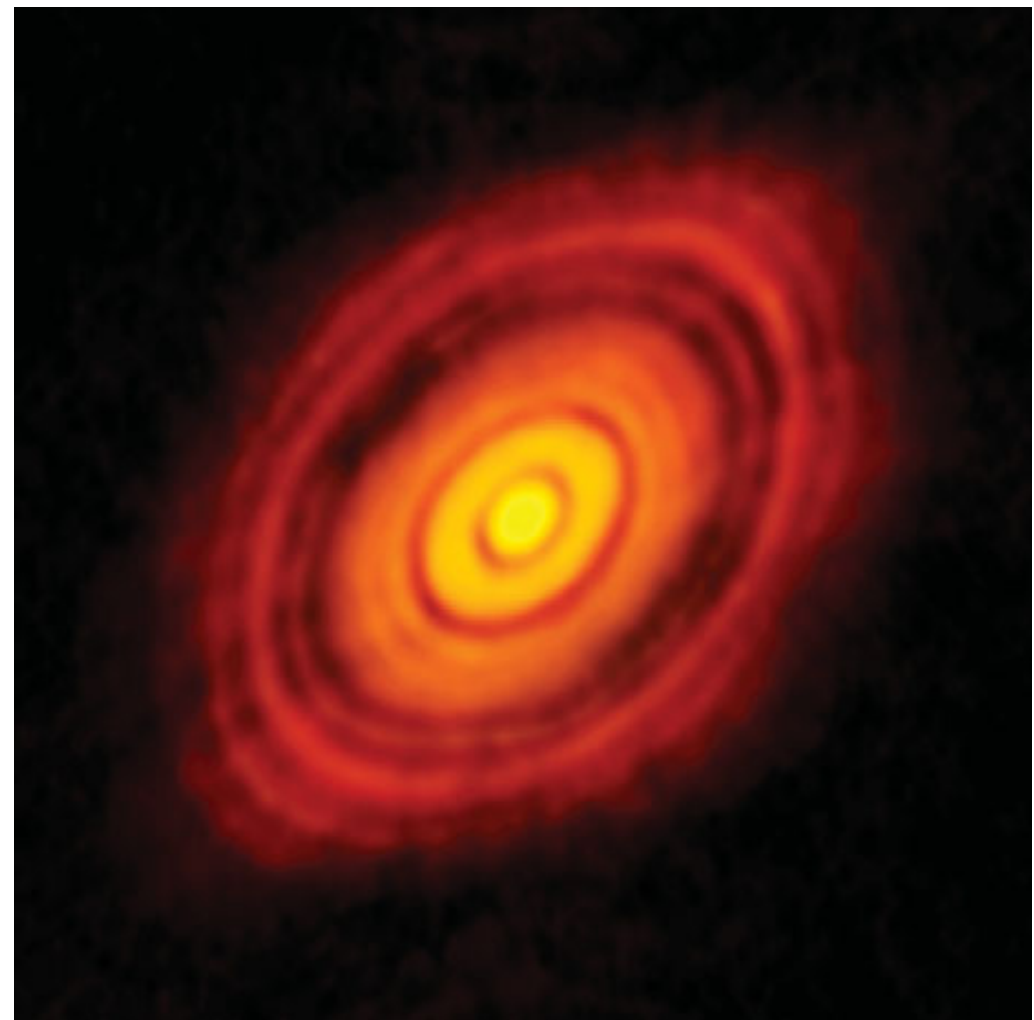
Origin of Planetary Systems

- The Nebular Model (basic ideas by Kant and Laplace)
 - The disk-formation process forms the basis for the “nebular model” for the formation of planetary systems, including our own solar system.
 - As a proto-stellar cloud collapses under the pull of its own gravity, conservation of its initial angular momentum leads naturally to form of an orbiting disk, which surrounds the central core mass.
 - This disk is initially gaseous, held **in a vertical hydrostatic equilibrium** about the disk mid-plane, **with radial support against gravity provided by the centrifugal force**.
 - This stops the rapid, dynamical infall, but as the viscous coupling between differentially rotating rings (and the entrainment of disk material by an outflowing stellar wind) transports angular momentum outward, there remains relatively slow inward diffuse flow of material that causes much of the initial disk mass to gradually accrete onto the young star.
 - This gradually depletes H and He gas (over a few million years). During this period, the heavier elements can gradually bond together to make molecules.
 - These in turn nucleate into grains of dust, and eventually into rocks.
 - Collisions among these rocks leads to a combination of fragmentation and accumulation, with the latter eventually forming asteroid-size (m to km) bodies. These then make planetoids, and eventually planets.



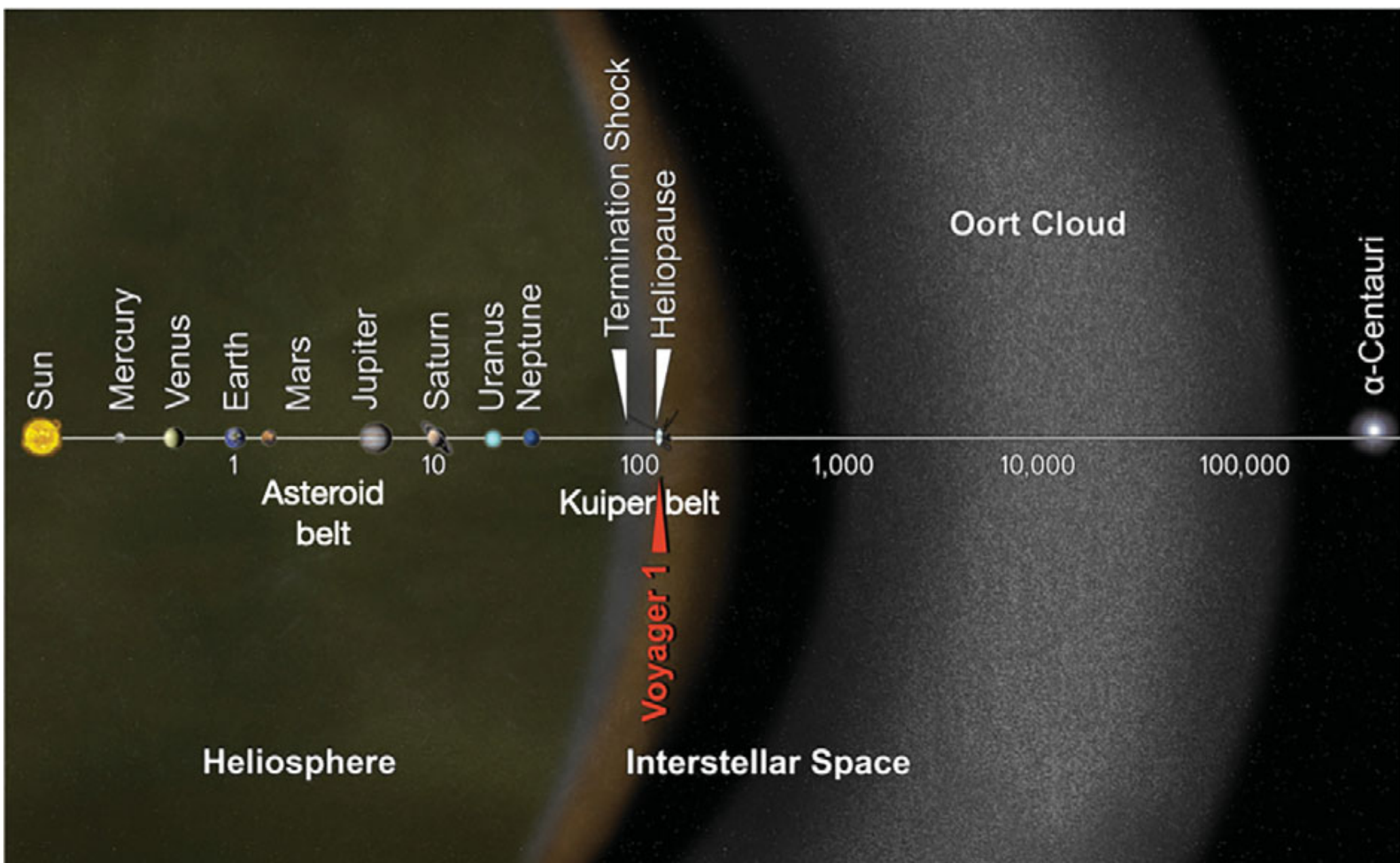
Observations of Proto-Planetary Disks

- Young stellar objects (YSOs) often show clear evidence of proto-planetary disks.
- With advent of telescope array (e.g., ALMA) observing in the far-IR and submm spectral regions, it is now becoming possible to image such disks directly.
- The figure shows an ALMA image of a proto-planetary disk in the T Tauri star HL Tauri, made in mm wavelengths.
- Interferometry from the array allows spatial resolution ranging down to 0.025 arcsec. At HL Tauri's distance of 140 pc, this corresponds to 3.5 AU, with the visible disk extending over a diameter of ~ 200 AU.
- The disk gaps likely represent regions where planet formation is clearing out disk debris, though there is so far no direct evidence of fully formed planets in this system.
- A key issue in planet formation is whether this can occur quickly enough to compete with disk depletion by various processes, like accretion onto the star, dissociation by stellar UV radiation, and entrainment in a outflowing stellar wind.



Our Solar System

- Planets
 - Rocky planets (rocky dwarfs; terrestrial planets): Mercury, Venus, Earth, Mars
 - Gas giants: Jupiter and Saturn
 - Ice giants: Uranus and Neptune



- **Snow line (also known as the ice line or frost line)**

- the particular distance in the solar nebula from the central protostar where it is cold enough for volatile compounds such as water, ammonia, methane, carbon dioxide, and carbon monoxide to condense into solid ice grains.

In the solar system, the distance for the snow line is ~ 3 AU, between Mars and Jupiter

- In the colder outer regions, these condensed to form ice, which gradually collected into ever larger solid cores, eventually growing massive enough to gravitationally attract and retain the even more abundant but lighter gases of hydrogen and helium.
 - ◆ This is the basis for formation of the outer gas and ice giant planets, with an overall composition similar to the solar nebula, and the present day Sun.
- In the inner nebula, where it was too warm to form ice, such light atoms of H and He escaped from the weaker gravity of the smaller, rocky planets, effectively preventing their growth and so keeping them relatively small.

- **Hot Jupiter**

- a planet with a mass comparable to (actually even larger than) Jupiter, but orbiting at such a close distance that the stellar heating would make it quite hot.
- Such gas giants had been supposed to form only beyond the ice line. The detection of hot Jupiters around several stars was a real surprise.
- They are thought to have formed outside the snow line, and later migrated inwards to their current positions. Gravitational interaction with the proto-stellar disk and/or other giant planets out there is supposed to lead some to be flung into an inward migration, so that they finally ended up very close to their star.

Equilibrium Temperature

- For an absorbing sphere with radius r at a distance d from the star, the intercepted flux of the stellar luminosity L_* is

$$\frac{\pi r^2 L_*}{4\pi d^2} = \pi r^2 \sigma_{\text{SB}} T_*^4 \left(\frac{R_*}{d} \right)^2$$

- where R_* and T_* are the star's radius and effective temperature, and σ_{SB} is the Stefan-Boltzmann constant.
- If we assume this sphere then radiates this energy as a blackbody over its surface area, then solving for its ***equilibrium temperature*** gives

$$\pi r^2 \sigma_{\text{SB}} T_*^4 \left(\frac{R_*}{d} \right)^2 = 4\pi r^2 \sigma_{\text{SB}} T_{\text{planet}}^4$$

$$T_{\text{planet}}(d) = T_* \sqrt{\frac{R_*}{2d}} \approx 280 \text{ K} \sqrt{\frac{1 \text{ AU}}{d}}$$

← $T_\odot = 5780 \text{ K}$
 $R_\odot = 6.9634 \times 10^5 \text{ km}$

Detection of Exoplanets (Extra-solar planets)

- Direct-Imaging Method

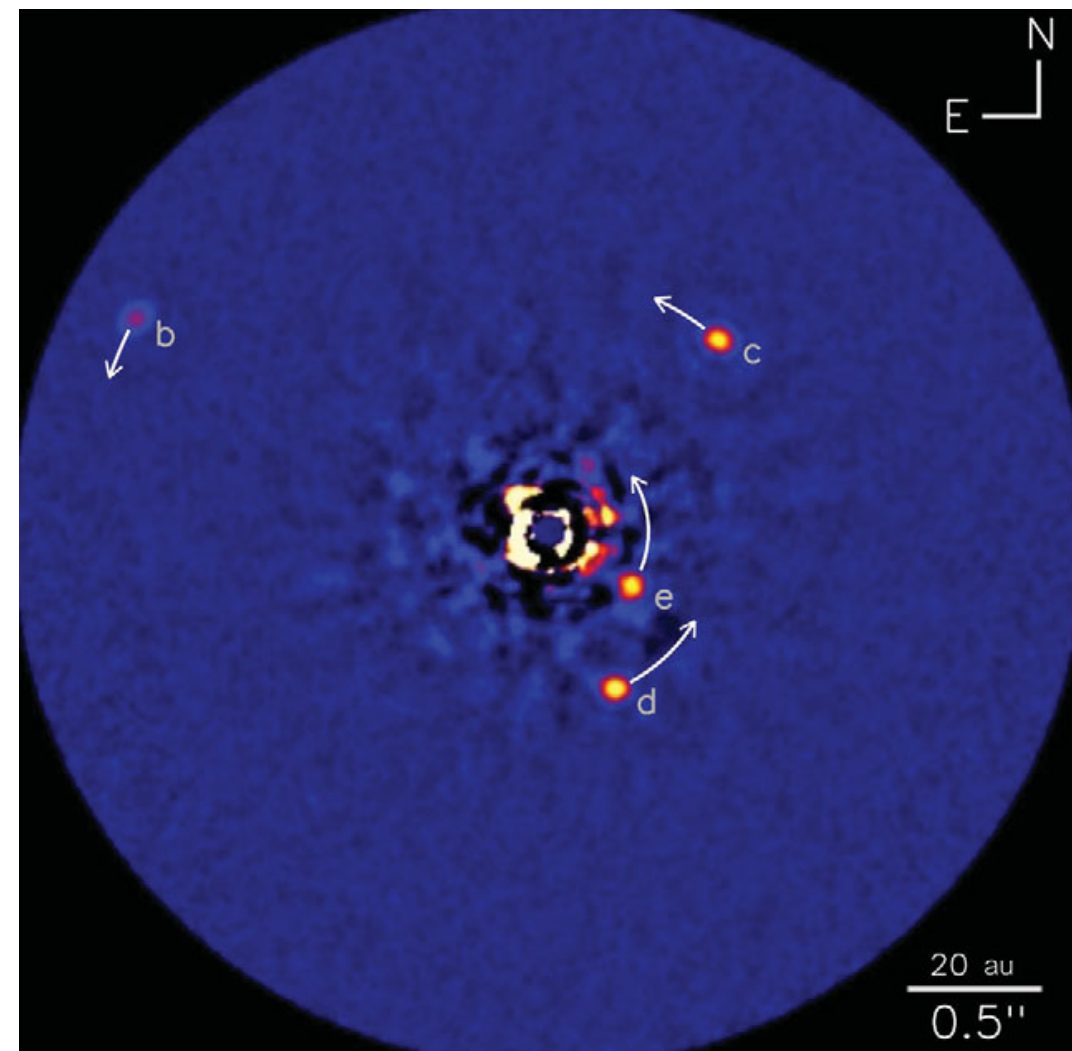
- Because they are much cooler than stars, the thermal emission from planets is mostly in the IR.
- Their appearance at visible wavelengths comes by reflected light from their host stars. This greatly complicates direct detection of extra-solar planets, since this reflected light is generally overwhelmed by the direct light from the stars.
- Nowadays, there are ~ 20 such detect imaging detections of exoplanets.

Direct image by the Keck Observatory of 4 exoplanets orbiting HR8799.

The arrows indicate their orbital motion from monitoring their positions over more than a decade. The orbital periods are 49, 100, 189, and 474 years for planets e, d, c, and b, respectively.

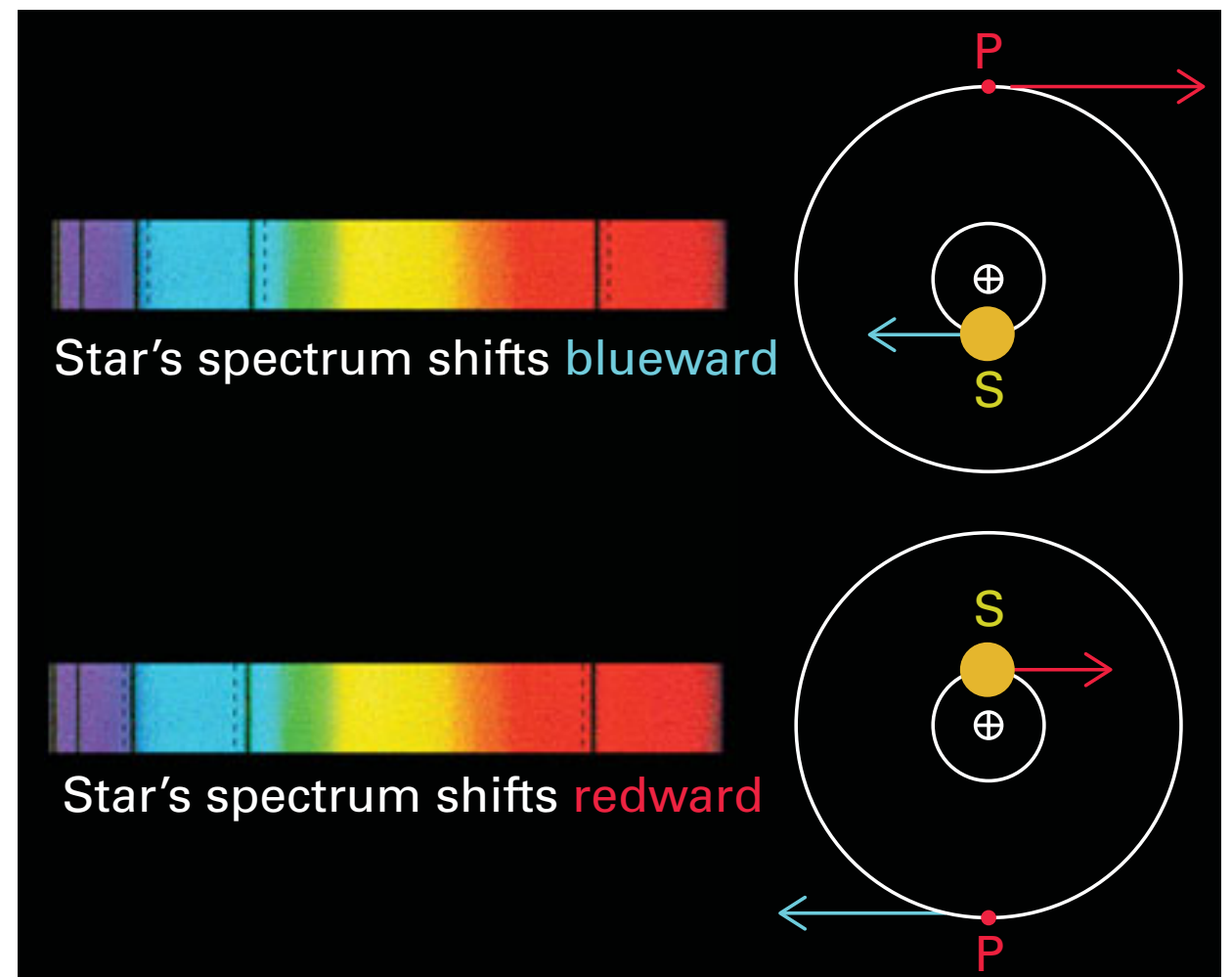
For reference, the orbital period of Neptune is 165 years.

[NTV-HIS/C. Marois/W. M. Keck Observatory]



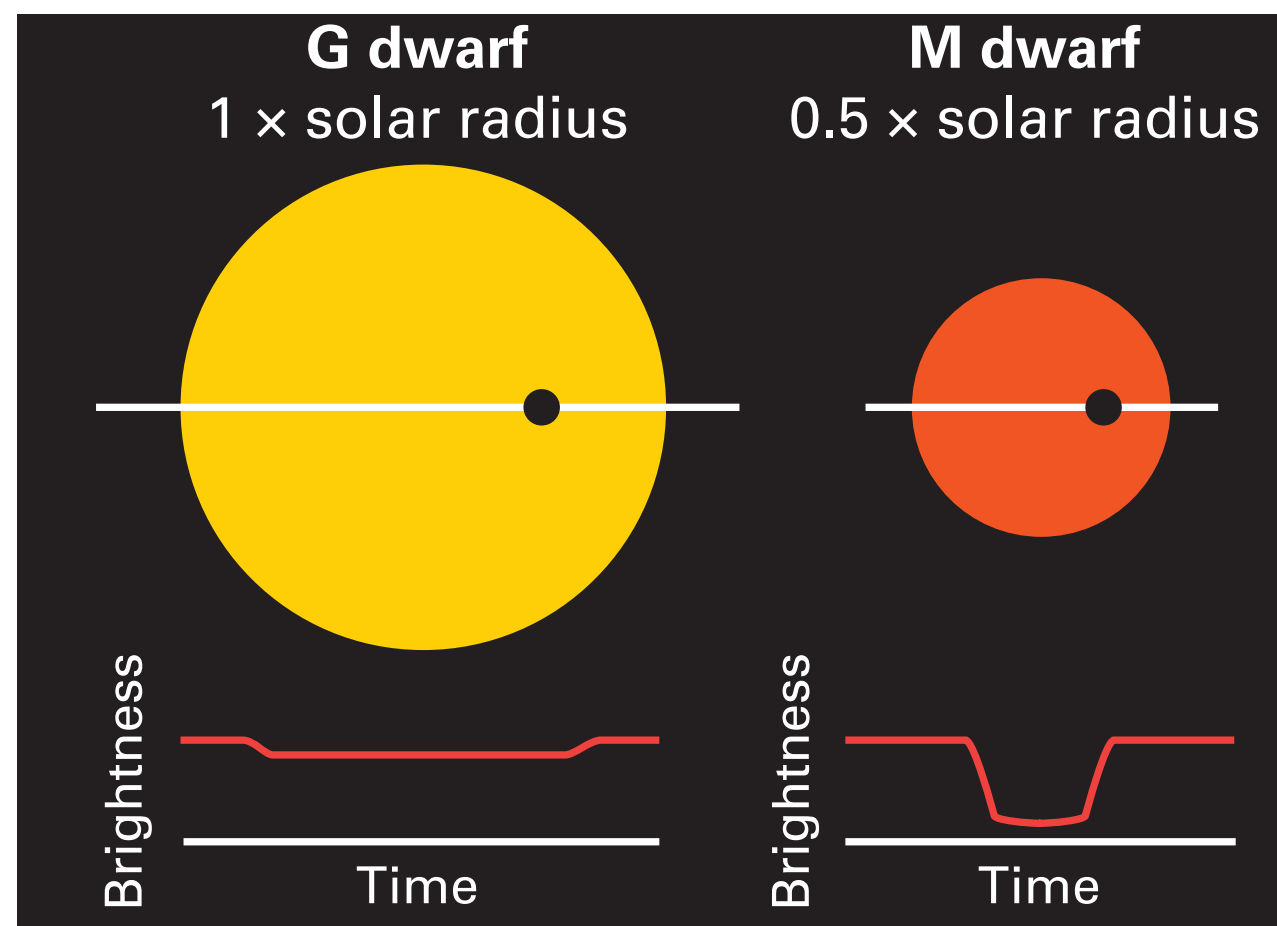
- Radial-Velocity Method

- The periodic movement of the host star due to the gravitational pull of the planet causes spatial “wobble.”
- This wobble is not directly detectable, but, its associated motion toward and away from the observer can be detected via very precise spectroscopic measurements of the systematic Doppler shift from multiple absorption lines in the star’s spectrum.
- This is the same method as used in spectroscopic binaries.



-
- **Transit Method**
 - This method simply looks for the slight dimming of the star's apparent brightness whenever a planet “transits” in front of it.
 - Instead of elaborate spectroscopic measurement of the slight Doppler shift, this merely requires precise photometric measurements of changes in the star's total apparent brightness. (This is analogous to eclipsing binaries)
 - The fractional drop in the star's brightness will be

$$\frac{\Delta F}{F} = \left(\frac{R_p}{R_*} \right)^2$$

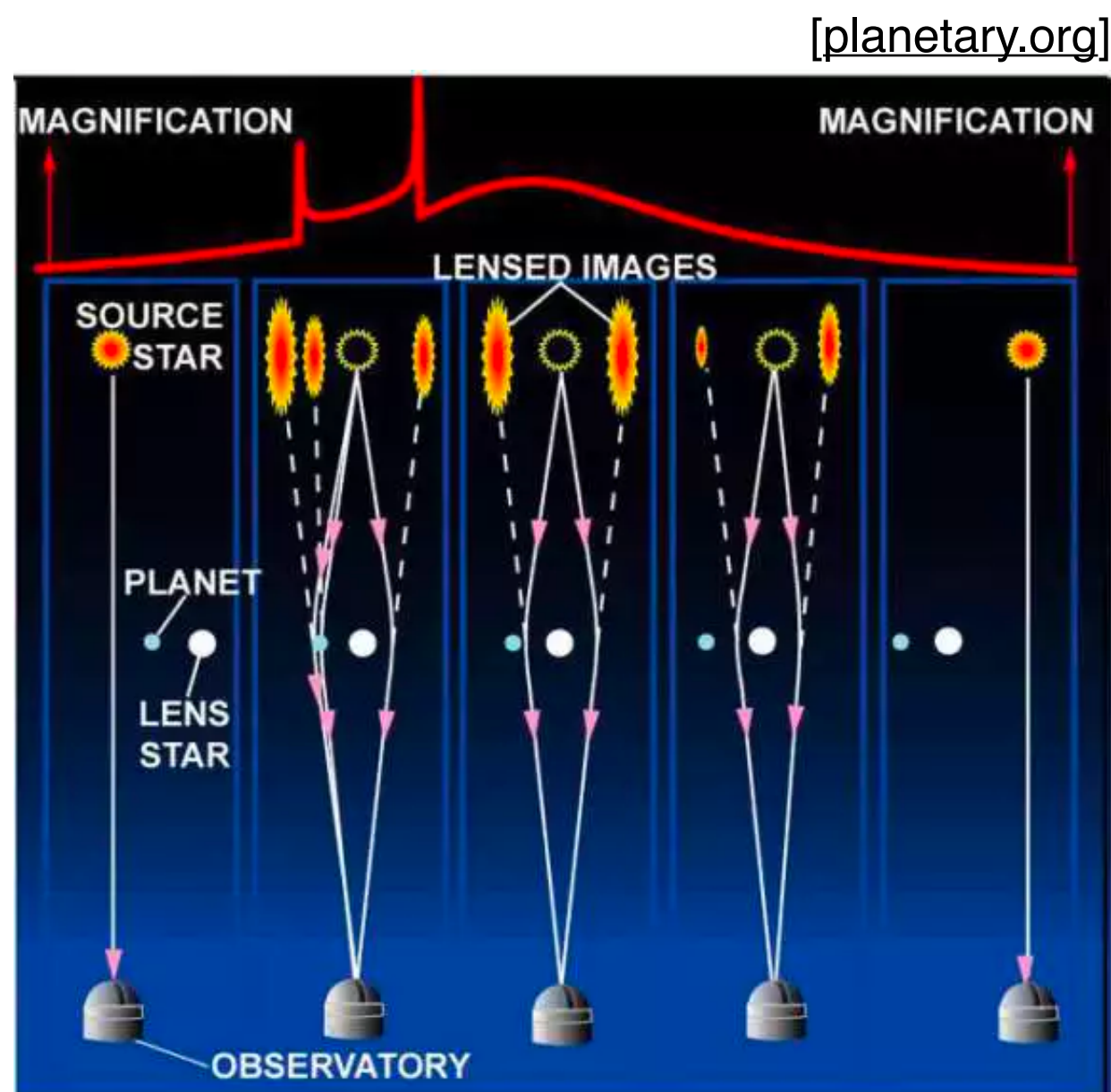


- Microlensing Method

- Microlensing is a form of gravitational lensing in which the light from a background source is bent by the gravitational field of a foreground lens to create distorted, multiple and/or brightened images.

The lensing star (white) moves in front of the source star (yellow) magnifying its image and creating a microlensing event.

In the second image (from left), the planet adds its own microlensing effect, creating the two characteristic spikes in the light curve.



Homework (due date: 04/11)

[Q5]

If the dust extinction A_λ were a power law in the wavelength, $A_\lambda \propto \lambda^{-\alpha}$, what would be R_V as a function of α ?

What value of α would give $R_V = 3.1$?

[Q6] - Virial Theorem

Read the section 2 of the following reference:

<https://www.uio.no/studier/emner/matnat/astro/nedlagte-emner/AST1100/h09/undervisningsmateriale/lecture5.pdf>

The above reference derives the potential energy for a spherical cloud with a uniform density.

(You can also read the section 1 for the proof of the Virial theorem.)

Consider a spherical cloud with a total mass M and a radius R . Assume that the cloud has a radial density profile of $\rho = \rho_0(r/R)^{-\beta}$. The gravitational potential energy can be expressed as follows:

$$U = -\alpha \frac{GM^2}{R}$$

- (a) For the above equation to be satisfied, what is the condition for β ?
- (b) Express α in terms of β .